

Babeş-Bolyai University Faculty of Chemistry and Chemical Engineering Supramolecular Organic and Organometallic Chemistry Centre



Contributions to the chemistry of late *d* metal complexes with multidentate ligands. Synthesis, structure and optical properties

PhD Thesis
Abstract

Darius Dumitraș

Scientific advisor: Prof. Dr. Anca Daniela Silvestru

Cluj-Napoca 2025

JURY

PRESIDENT:

Prof. Dr. Niculina Daniela Hădade

Babeș-Bolyai University, Cluj-Napoca, Romania

SCIENTIFIC ADVISOR:

Prof. Dr. Anca Daniela Silvestru

Babeș-Bolyai University, Cluj-Napoca, Romania

REVIEWERS:

Dr. Esteban Pablo Urriolabeitia, Investigador Científico

Universidad de Zaragoza, Zaragoza, Spain

Acad. Marius Andruh

University of Bucharest, Bucharest, Romania

Prof. Dr. Gabriela-Nicoleta Nemeș

Babeş-Bolyai University, Cluj-Napoca, Romania

TABLE OF CONTENTS

I.	INTR	ODUCTION	11
II.	LITE	RATURE DATA	13
II.1.	Orga	anoselenium fluorophores	13
II	.1.1.	Applications	13
II	.1.2.	Synthesis and structural characterization	16
	II.1.2.1	1. Diorganoselenium(II) compounds of type R–Se–R'	16
	II.1.2.2	2. Diorganoselenium(II) compounds of type R–Se–CH ₂ –Py–CH ₂ –Se–R	24
II.2.	Imio	dazolone and thiazolone fluorophores	29
II	.2.1.	Applications	29
II	.2.2.	Synthesis and structural characterization	33
III.	ORIG	GINAL CONTRIBUTIONS	40
Ove	rview		40
III.1	. Orga	anoselenium compounds	41
II	I.1.1.	Diorganoselenium(II) compounds of type R-Se-R	41
	III.1.1.	.1. Synthesis and structural characterization	41
	III.1.1.	.2. Evaluation of optical properties	48
	III.1.1.	.3. Conclusions	49
II	I.1.2.	Metal complexes of diorganoselenium(II) ligands of type R-Se-R	50
	III.1.2.	.1. Synthesis and structural characterization	50
	III.1.2.	2.2. Evaluation of optical properties	60
	III.1.2.	3. Conclusions	61
II	I.1.3.	Diorganoselenium(II) compounds of type R-Se-CH ₂ -Py-CH ₂ -Se-R	62
	III.1.3.	.1. Synthesis and structural characterization	62
	III.1.3.	.2. Evaluation of optical properties	69
	III.1.3.	.3. Conclusions	69
II	I.1.4.	Metal complexes of diorganoselenium(II) ligands of type R–Se–CH ₂ –Py–CH ₂ –Se–R	70
	III.1.4.	.1. Synthesis and structural characterization	70
	III.1.4.	.2. Evaluation of optical properties	84
	III.1.4.	-3. Conclusions	85
III.2	. Imic	dazolone and thiazolone based compounds	87
II	I.2.1.	Imidazolones and thiazolones	87
	III 2 1	1 Synthesis and structural characterization	87

III.2.1.2	2. Conclusions	91
III.2.2.	Orthopalladated imidazolones and thiazolones	91
III.2.2.1	1. Synthesis and structural characterization	91
III.2.2.2	2. Evaluation of the optical properties	109
III.2.2.3	3. Computational calculations	112
III.2.2.4	4. Conclusions	113
IV. EXPER	RIMENTAL	114
IV.1. Gene	eral information	114
IV.2. Synth	hesis of diorganoselenium(II) compounds of type R-Se-R	117
Synthesis	of {2-[(CH ₂ O) ₂ CH]C ₆ H ₄ } ₂ Se (1) ¹²⁴	117
Synthesis of	of {4-[(CH ₂ O) ₂ CH]C ₆ H ₄ } ₂ Se (2) ¹²⁴	118
Synthesis	of {2-(OCH)C ₆ H ₄ } ₂ Se (3)	119
Synthesis	of {4-(OCH)C ₆ H ₄ } ₂ Se (4)	120
Synthesis	of [(Z)-2-{2-C ₆ H ₅ -oxazol-5(4 <i>H</i>)-one}CHC ₆ H ₄] ₂ Se (5)	121
Synthesis	of [(Z)-4-{2-C ₆ H ₅ -oxazol-5(4 <i>H</i>)-one}CHC ₆ H ₄] ₂ Se (6)	122
IV.3. Syntl	hesis of metal complexes of diorganoselenium(II) ligands of type R-	Se–R 123
Synthesis of	of $[Ag\{[(Z)-2-\{2-C_6H_5-oxazol-5(4H)-one\}CHC_6H_4]_2Se\}][OTf]$ (7)	123
Synthesis	of $[Ag\{[(Z)-4-\{2-C_6H_5-oxazol-5(4\mathit{H})-one\}CHC_6H_4]_2Se\}][OTf]$ (8)	124
Synthesis of	of $[Ag_2\{[(Z)-2-\{2-C_6H_5-oxazol-5(4H)-one\}CHC_6H_4]_2Se\}][OTf]_2$ (9))125
Synthesis of	of $[Ag_2\{[(Z)-4-\{2-C_6H_5-oxazol-5(4H)-one\}CHC_6H_4]_2Se\}][OTf]_2$ (10))) 126
Synthesis of	of $[Ag\{[(Z)-2-\{2-C_6H_5-oxazol-5(4H)-one\}CHC_6H_4]_2Se\}][PF_6]$ (11).	127
Synthesis of	of $[Ag\{[(Z)-4-\{2-C_6H_5-oxazol-5(4H)-one\}CHC_6H_4]_2Se\}][PF_6]$ (12).	128
Synthesis of	of $[AuC1\{[(Z)-2-\{2-C_6H_5-oxazol-5(4H)-one\}CHC_6H_4]_2Se\}]$ (13)	129
Synthesis of	of $[AuC1\{[(Z)-4-\{2-C_6H_5-oxazol-5(4H)-one\}CHC_6H_4]_2Se\}]$ (14)	130
Synthesis of	of $[ZnCl_2\{[(Z)-2-\{2-C_6H_5-oxazol-5(4H)-one\}CHC_6H_4]_2Se\}]$ (15)	131
Synthesis of	of $[ZnCl_2\{[(Z)-4-\{2-C_6H_5-oxazol-5(4H)-one\}CHC_6H_4]_2Se\}]$ (16)	132
IV.4. Synth	hesis of the diorganodiselenides	133
	of [HOC(CH ₃) ₂ CH ₂] ₂ Se ₂ (17)	
Synthesis of	of (C ₅ H ₄ N) ₂ Se ₂ (18) ¹³⁷	134
Synthesis	of [2-(C ₃ H ₃ N ₂)CH ₂ CH ₂] ₂ Se ₂ (19) ¹³⁶	135
•	hesis of diorganoselenium(II) compounds type e-CH ₂ -Py-CH ₂ -Se-R	136
	of {2-[HOC(CH ₃) ₂ CH ₂]SeCH ₂ } ₂ Py (20)	
-	of [2-(C ₅ H ₄ N)SeCH ₂] ₂ Py (21)	
	of [2-(C ₃ H ₃ N ₂)CH ₂ CH ₂ SeCH ₂] ₂ Pv (22)	

IV.6.	Synthesis of metal complexes of diorganoselenium(II) ligands of type R–Se–CH ₂ –Py–CH ₂ –Se–R	139
Syı	rnthesis of [Ag{2-[HOC(CH ₃) ₂ CH ₂]SeCH ₂ } ₂ Py][OTf] (23)	139
	rnthesis of [Ag{2-(C ₅ H ₄ N)SeCH ₂ } ₂ Py][OTf] (24)	
	nthesis of [Ag{2-(C ₃ H ₃ N ₂)CH ₂ CH ₂ SeCH ₂]} ₂ Py][OTf] (25)	
	nthesis of $[Ag\{2-(C_5H_4N)SeCH_2\}_2Py][PF_6]$ (26)	
Syı	rnthesis of [Ag{2-(C ₃ H ₃ N ₂)CH ₂ CH ₂ SeCH ₂]} ₂ Py][PF ₆] (27)	143
	rnthesis of [Ag{2-(C ₅ H ₄ N)SeCH ₂ } ₂ Py][NO ₃] (28)	
Syı	rnthesis of [Ag{2-(C ₃ H ₃ N ₂)CH ₂ CH ₂ SeCH ₂]} ₂ Py][NO ₃] (29)	145
Syı	rnthesis of [CuI{2-(C ₅ H ₄ N)SeCH ₂ } ₂ Py] (30)	146
Syı	rnthesis of [CuI{2-(C ₃ H ₃ N ₂)CH ₂ CH ₂ SeCH ₂]} ₂ Py] (31)	147
IV.7.	Synthesis of oxazolones	148
Sy	enthesis of (Z)-4-(4-FC ₆ H ₄ CH)-2-C ₆ H ₅ -oxazol-5(4 <i>H</i>)-one (32) ¹⁴⁵	148
Sy	nthesis of (Z)-4-(4-ClC ₆ H ₄ CH)-2-C ₆ H ₅ -oxazol-5(4 <i>H</i>)-one (33) ¹⁴⁶	148
Sy	enthesis of (Z)-4-(3,4-Cl ₂ C ₆ H ₃ CH)-2-C ₆ H ₅ -oxazol-5(4 <i>H</i>)-one (34) ¹⁴⁷	149
Syı	enthesis of (Z)-4-[3,4-(CH ₃ O) ₂ C ₆ H ₃ CH]-2-C ₆ H ₅ -oxazol-5(4 <i>H</i>)-one (35) ¹⁴⁸	149
Syı	enthesis of (Z)-4-[2,4-(CH ₃ O) ₂ C ₆ H ₃ CH]-2-C ₆ H ₅ -oxazol-5(4 <i>H</i>)-one (36) ¹⁴⁹	150
IV.8.	Synthesis of imidazolones	151
Syı	nthesis of (Z)-4-(4-FC ₆ H ₄ CH)-1-CH ₂ CH ₂ CH ₃ -2-C ₆ H ₅ -imidazol-5(4 <i>H</i>)-one (37) 151
Syı	nthesis of (Z)-4-(4-ClC ₆ H ₄ CH)-1-CH ₂ CH ₂ CH ₃ -2-C ₆ H ₅ -imidazol-5(4 <i>H</i>)-one (3 8)	8) 152
Syı	$ \text{ nthesis of (Z)-4-(3,4-Cl}_2\text{C}_6\text{H}_3\text{CH})-1-\text{CH}_2\text{CH}_2\text{CH}_3-2-\text{C}_6\text{H}_5-\text{imidazol-5}(4\textit{H})-\text{one } \\$	(39)153
•	rnthesis of)-4-[3,4-(CH ₃ O) ₂ C ₆ H ₃ CH]-1-CH ₂ CH ₂ CH ₃ -2-C ₆ H ₅ -imidazol-5(4 <i>H</i>)-one (40)	154
•	nthesis of	
)-4-[2,4-(CH ₃ O) ₂ C ₆ H ₃ CH]-1-CH ₂ CH ₂ CH ₃ -2-C ₆ H ₅ -imidazol-5(4 <i>H</i>)-one (41)	
IV.9.	•	
_	in the sis of (Z)-4-(4-FC ₆ H ₄ CH)-2-C ₆ H ₅ -thiazol-5(4 <i>H</i>)-one (42) ¹⁴⁴	
	in the sis of (Z)-4-(4-ClC ₆ H ₄ CH)-2-C ₆ H ₅ -thiazol-5(4 <i>H</i>)-one (43) ¹⁴⁴	
-	enthesis of (Z)-4-(3,4-Cl ₂ C ₆ H ₃ CH)-2-C ₆ H ₅ -thiazol-5(4 <i>H</i>)-one (44) ¹⁴⁴	
	enthesis of (Z)-4-[3,4-(CH ₃ O) ₂ C ₆ H ₃ CH]-2-C ₆ H ₅ -thiazol-5(4 <i>H</i>)-one (45) ¹⁴⁴	
Sy	enthesis of (Z)-4-[3,4-(CH ₃ O) ₂ C ₆ H ₃ CH]-2-C ₆ H ₅ -thiazol-5(4 <i>H</i>)-one (46) ¹⁴⁴	
IV.10	1	
-	nthesis of $[Pd_2\{\kappa^2(C,N)-(Z)-4-(4-FC_6H_3CH)-1-CH_2CH_2CH_3-2-C_6H_5-imidazol-e\}_2(\mu\text{-OOCCF}_3)_2]$ (47)	
	rnthesis of $[Pd_2\{\kappa^2(C,N)-(Z)-4-(4-ClC_6H_3CH)-1-CH_2CH_2CH_3-2-C_6H_5-imidazole\}$ (u-OOCCF ₃) ₂] (48)	

VI.	REFERENCES	180
V.	CONCLUSIONS	178
	Synthesis of $[Pd{\kappa^2(C,N)-(Z)-4-[2,4-(CH_3O)_2C_6H_2CH]-1-CH_2CH_2CH_3-2-C_6H_5-imidat_5(4H)-one}(NC_5H_5)(NC_5H_5)][BF_4]$ (65)	177
	Synthesis of [Pd{ κ^2 (C,N)-(Z)-4-[2,4-(CH ₃ O) ₂ C ₆ H ₂ CH]-1-CH ₂ CH ₂ CH ₃ -2-C ₆ H ₅ -imida: 5(4 <i>H</i>)-one} { κ^2 (O,O)-([CH ₃ C(O)] ₂ CH ₂)}] (64)	176
	Synthesis of $[Pd{\kappa^2(C,N)-(Z)-4-[2,4-(CH_3O)_2C_6H_2CH]-1-CH_2CH_2CH_3-2-C_6H_5-imidat_5(4H)-one}(Cl)(NC_5H_5)]$ (63)	175
	Synthesis of $[Pd_2\{\kappa^2(C,N)-(Z)-4-[2,4-(CH_3O)_2C_6H_2CH]-1-CH_2CH_2CH_3-2-C_6H_5-imidazol-5(4\emph{H})-one}_2(\mu-Cl)_2]$ (62)	
	Synthesis of $[Pd{\kappa^2(C,N)-(Z)-4-[2,4-(CH_3O)_2C_6H_2CH]-1-CH_2CH_3-2-C_6H_5-imidat_5(4H)-one}(OOCCF_3)(NC_5H_5)]$ (61)	
Γ	V.13. Synthesis of orthopalladated imidazolone analogs	
	Synthesis of $[Pd_2\{\kappa^2(C,N)-(Z)-4-(3,4-Cl_2C_6H_3CH)-2-C_6H_5-thiazol-5(4H)-one\}_2(\mu-OOCCF_3)_2]$ cyclobutane derivative (60)	172
	Synthesis of $[Pd_2\{\kappa^2(C,N)-(Z)-4-(4-ClC_6H_3CH)-2-C_6H_5-thiazol-5(4H)-one\}_2(\mu-OOCCF_3)_2]$ cyclobutane derivative (59)	171
	Synthesis of $[Pd_2\{\kappa^2(C,N)-(Z)-4-(3,4-Cl_2-ClC_6H_3CH)-1-CH_2CH_2CH_3-2-C_6H_5-imidaze 5(4H)-one\}_2(\mu-OOCCF_3)_2]$ cyclobutane derivative (58)	
	Synthesis of $[Pd_2\{\kappa^2(C,N)-(Z)-4-(4-ClC_6H_3CH)-1-CH_2CH_2CH_3-2-C_6H_5-imidazol-5(4L_6H_3CH)-1-CH_2CH_3-2-C_6H_5-imidazol-5(4L_6H_3CH)-1-CH_2CH_3-2-C_6H_3-imidazol-5(4L_6H_3CH)-1-CH_2CH_3-2-C_6H_3-imidazol-5(4L_6H_3CH)-1-CH_2CH_3-2-C_6H_3-imidazol-5(4L_6H_3CH)-1-CH_2CH_3-2-C_6H_3-2-C$	-
	Synthesis of $[Pd_2\{\kappa^2(C,N)-(Z)-4-(4-FC_6H_3CH)-1-CH_2CH_2CH_3-2-C_6H_5-imidazol-5(4H_5)-(\mu-OOCCF_3)_2]$ cyclobutane derivative (56)	
Γ	V.12. Synthesis of cyclobutane derivatives	
	Synthesis of $[Pd_2\{\kappa^2(C,N)-(Z)-4-[3,4-(CH_3O)_2C_6H_2CH]-2-C_6H_5$ -thiazol-5(4 <i>H</i>)-one $\}_2(OOCCF_3)_2]$ (55)	μ-
	Synthesis of $[Pd_2\{\kappa^2(C,N)-(Z)-4-(3,4-Cl_2C_6H_3CH)-2-C_6H_5-thiazol-5(4H)-one\}_2(\mu-OOCCF_3)_2]$ (54)	166
	Synthesis of $[Pd_2\{\kappa^2(C,N)-(Z)-4-(4-ClC_6H_3CH)-2-C_6H_5-thiazol-5(4\emph{H})-one\}_2(\mu-OOCCF_3)_2]$ (53)	165
	Synthesis of $[Pd_2{\kappa^2(C,N)-(Z)-4-(4-FC_6H_3CH)-2-C_6H_5-thiazol-5(4\it{H})-one}_2(\mu-OOCCF_3)_2]$ (52)	164
Γ	V.11. Synthesis of orthopalladated thiazolones	164
	Synthesis of $[Pd_2\{\kappa^2(C,N)-(Z)-4-[2,4-(CH_3O)_2C_6H_2CH]-1-CH_2CH_2CH_3-2-C_6H_5-imidazol-5(4H)-one\}_2(\mu-OOCCF_3)_2]$ (51)	163
	Synthesis of $[Pd_2\{\kappa^2(C,N)-(Z)-4-[3,4-(CH_3O)_2C_6H_2CH]-1-CH_2CH_2CH_3-2-C_6H_5-imidazol-5(4\emph{H})-one}_2(\mu-OOCCF_3)_2]$ (50)	162
	Synthesis of [Pd ₂ { κ^2 (C,N)-(Z)-4-(3,4-Cl ₂ -ClC ₆ H ₃ CH)-1-CH ₂ CH ₂ CH ₃ -2-C ₆ H ₅ -imidaze 5(4 <i>H</i>)-one} ₂ (μ -OOCCF ₃) ₂] (49)	

VII.	APPENDIX		
VIII.	RES	SULTS DISSEMINATION	194
VIII.	1.	List of articles	194
VIII.	2.	List of conferences	194
ACKN	OW	LEDGEMENTS	195

I. INTRODUCTION

In more recent times fluorescence has been proven an important tool and used in many applications such as fluorescent lamps,⁵ fluorescent spectroscopy,^{6,7} fluorescence imaging,^{8,9} photodynamic therapy,¹¹ pigments^{12,13} and detection of fingerprints.¹⁴

Considering the previous applications of fluorescent compounds, in this work we synthesized a series of organoselenium compounds. Such species were used as ligands towards late d metals (Ag, Pd), and, for selected species, the fluorescent behaviour was investigated to evaluate their potential for applications optoelectronics.

The first part of the original contributions focused on the organoselenium compounds. The diorganoselenides were further divided by their overall structure in compounds of type R—Se—R, where one selenium atom is attached to two identic units of either benzaldehyde or 4-arylidene-5(4*H*)-oxazolone fragments, and compounds of type R—Se—CH₂—Py—CH₂—Se—R, where a pyridine ring is functionalized with two flexible organoselenium side arms. The diorganoselenides R—Se—R were used as ligands for silver(I), gold(I) and zinc(II) complexes, while the R—Se—CH₂—Py—CH₂—Se—R ligands were used for silver(I) and copper(I) complexes.

The second part of the original contributions discuses a series of 4-arylidene-5(4*H*)-imidazolones and 4-arylidene-5(4*H*)-thiazolones. Palladium complexes of these ligands were obtained by C–H bond activation and were also investigated for their photophysical properties and photochemical reactivity.

II. LITERATURE DATA

II.1. Organoselenium fluorophores

In the past decade, the development of organoselenium compounds as fluorescent probes has attracted some interest. The most recent studies in the field are focused on their applications in bioimaging. As a consequence, diorganoselenium compounds containing donor atoms such as N and/or O were synthesized for the purpose of detecting biologically important analytes, such as reactive oxygen species (hydrogen peroxide, hypochlorous acid, hypobromous acid, superoxides, peroxynitrite and nitric oxide), biothiols and metal ions. ¹⁵⁻⁴²

One of the reasons to employ the organoselenium compounds as fluorophores is related to the chemical properties of selenium. In the divalent state, selenium can either weakly donate a lone electron pair to a metal center, thus behaving as a Lewis base, or to accept a lone pair from a donor atom and behaving as a Lewis acid.⁴³ In addition, selenium has a low oxidation potential which favors the reaction and detection of oxidizing reagents.⁴⁴

II.2. Imidazolone and thiazolone fluorophores

The green fluorescent protein (GFP), a 4-arylidene-5(4*H*)-imidazolone, is a protein that exhibits a bright green emission when it is irradiated with UV light. In was first found in some species of fluorescent jellyfish. Because the protein can be attached to the DNA it has been used as fluorescent indicator in a variety of living organisms.^{75,76} Most common applications are: fusion tags, reporter gene, fluorescence resonance energy transfer and photobleaching. Fusion tag is a method used to tag proteins. GFP is attached to a gene which when expression occurs in a cell it will propagate the fluorescence in future proteins. Reporter gene is used to mark a living organism and provides information regarding if a certain gene has been expressed in the cell or organism population.⁷⁷

Because of some limitations or the need to improve the fluorescence of GFP protein, synthetic analogs containing the same core structure of the GFP have been developed. These imidazolones are widely used and commercially available.⁸⁵ In an attempt to obtain compounds with specific applications attempts have been made to improve the already known GFP-like compounds, starting from the core structure of GFP.⁸⁶⁻¹⁰⁰

The luminescent properties of 4-arylidene-5(4*H*)-imidazolone are strongly dependent on the environment. It was observed that the quantum yield of the isolated imidazolone is much smaller when it is localized in GFP protein, due to the influence of a rigid environment. ^{101,102} The most likely reason for this behavior is the presence of non-radiative decay channels determined by Z-E isomerization, as an alternative to fluorescence. This isomerization can take place through rotation around the C=C bond and/or C-C bond. ^{103,104} With the introduction of substituents at specific positions the isomerization can be avoided through self-restrictions, intramolecular locks or ortho-functionalization. ^{106,105-110}

III. ORIGINAL CONTRIBUTIONS

III.1. Organoselenium compounds

III.1.1. Diorganoselenium(II) compounds of type R-Se-R

The synthesis of the benzaldehyde derivatives was achieved according to **Scheme 27**. $\{2-[(CH_2O)_2CH]C_6H_4\}_2Se$ (1) and $[2-(OCH_2)C_6H_4]_2Se$ (3) have been prepared according to a procedure described in the literature, while the new diorganoselenides $\{4-[(CH_2O)_2CH]C_6H_4\}_2Se$ (2) and $[4-(OCH_2)C_6H_4]_2Se$ (4) have been prepared by adapting the same literature procedure. 4-Bromobenzaldehyde was converted into the corresponding acetal. An *ortho*-lithiation step of the organic ligand was employed next. The resulting lithium derivative $\{4-[(CH_2O)_2CH]C_6H_4\}_2Li$ was reacted with $Se(dtc)_2$ (dtc = dimethyl dithiocarbamate), thus resulting the desired diorganoselenide 2. The compound $[4-(OCH_2)C_6H_4]_2Se$ (4) was prepared by reacting $\{4-[(CH_2O)_2CH]C_6H_4\}_2Se$ (2) with HCl, at reflux (**Scheme 27**).

Scheme 27. Synthetic path for benzaldehyde derivatives.

4-Arylidene-5(4*H*)-oxazolones were prepared as followings: the compounds [4-{2- C_6H_5 -(4*H*)-oxazol-5-onă} C_6H_4]₂Se (**5**) and [4-{2- C_6H_5 -(4*H*)-oxazol-5-onă} C_6H_4]₂Se (**6**) were obtained using the Erlenmeyer-Plöchl method by reacting the aldehydes [2-(OCH₂) C_6H_4]₂Se (**3**) and [4-(OCH₂) C_6H_4]₂Se (**4**), respectively, with hippuric acid and sodium acetate at reflux in acetic anhydride (**Scheme 28**). 125

Se
$$R_2$$
 R_2 R_2 R_2 P_2 P_3 P_4 P_4 P_5 P_5 P_6 P_6 P_7 P_8 P_8 P_8 P_9 P

Scheme 28. Synthetic path for compounds 5 and 6.

NMR spectroscopy was used to check the purity of 1 and 3, which have already been reported in the literature.¹²⁴ In the the ¹H NMR spectra of compounds 2, 4, 5 and 6 all the

resonance signals corresponding to the specific functional groups where found (**Figure 26**). In the spectrum of compound **2**, the resonance signals corresponding to the dioxolane group (δ 4.10 ppm) and the proton in position 7 (δ 5.80 ppm) are observed. In the spectrum of compound **4**, the resonance signals of the dioxolane group are no longer present, thus indicating that the deprotection was successful. Also, the resonance signal of the H₇ proton moves to δ 10.00 ppm, a value specific to an aldehyde group. In the spectrum of compound **6**, the proton in position 7 moved to a value characteristic for oxazolones (δ 7.24 ppm).

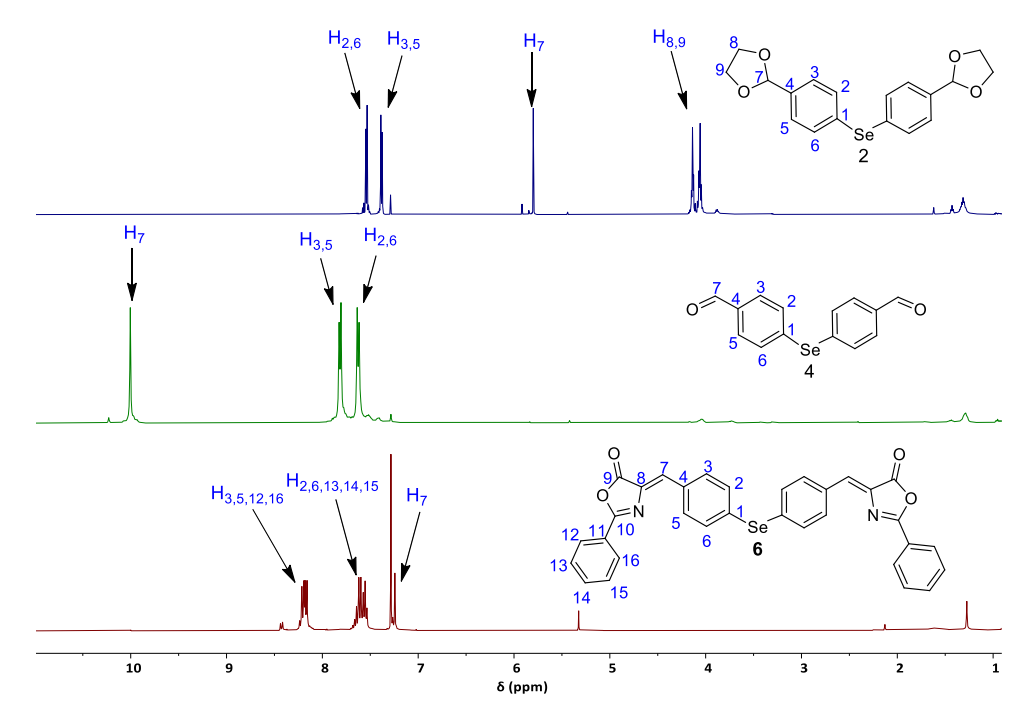


Figure 26. Stacked ¹H NMR spectra, in CDCl₃ solutions, of compounds 2, 4 and 6.

The ⁷⁷Se NMR spectra of compounds **2**, **4**, **5** and **6** revealed the resonances of the compounds (δ 415 ppm, 444 ppm, 438 ppm and 344 ppm, respectively) are close to those reported in literature for compounds **1** and **3** (δ 321 ppm and 393 ppm). ¹²⁴

In the APCI+ mass spectrum of compound **4**, **5** and **6** the pseudo-molecular ion [M+H]⁺ was found and confirmed the formation of the target species.

The compounds were further investigated by infrared spectroscopy. In the case of compound 4, the C–H and the C=O stretching bands of the aldehyde were identified and in the case of compounds 5 and 6 the bands corresponding to the oxazolone ring, C=O, C–O and C=N stretching band were also identified.

The molecular structures of compounds 4 and 5 were determined by single crystal X-ray diffraction. In compound 4 the bond angle around the selenium lead to a bent geometry with a value comparable to those found in diphenyl selenide. ¹²⁶ In the molecular structure of

compound **5** an angular geometry around the selenium atom is observed as well (**Figure 35**). The organic substituents attached to selenium are planar and almost orthogonal to each other.

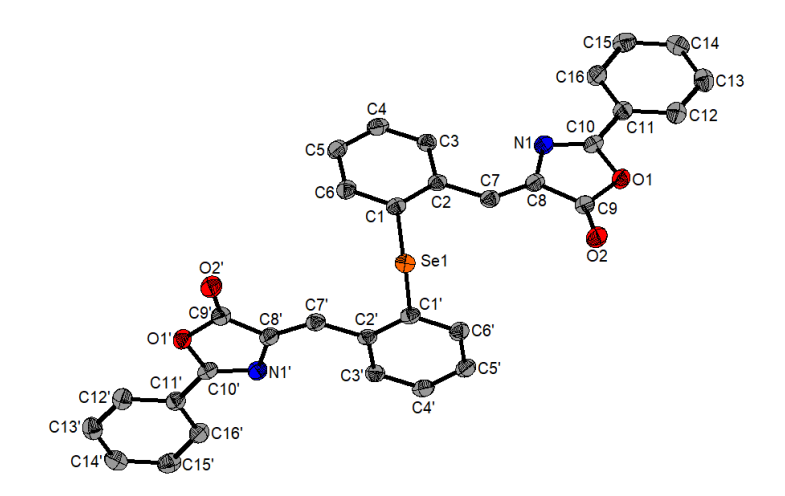


Figure 35. ORTEP representation (30% probability ellipsoids) of a molecule in compound **5**. Hydrogen atoms were omitted for clarity.

The UV-Vis spectroscopy investigations showed an increase of intensity of the 350 nm band in oxazolone 5 compared to benzaldehyde 3 and in case of compound 6, it showed a shift of the 320 nm band to 400 nm compared to compound 4 due to the extended conjugated system. The intensive absorption bands below 300 nm were assigned to intraligand π – π * interactions. Comparing the two oxazolones 5 and 6 (Figure 37), it can be observed that the position of selenium on the phenyl ring (ortho in compound 5 and para in compound 6) has a significant effect on the absorbance of the compounds, inducing a bathochromic shift.

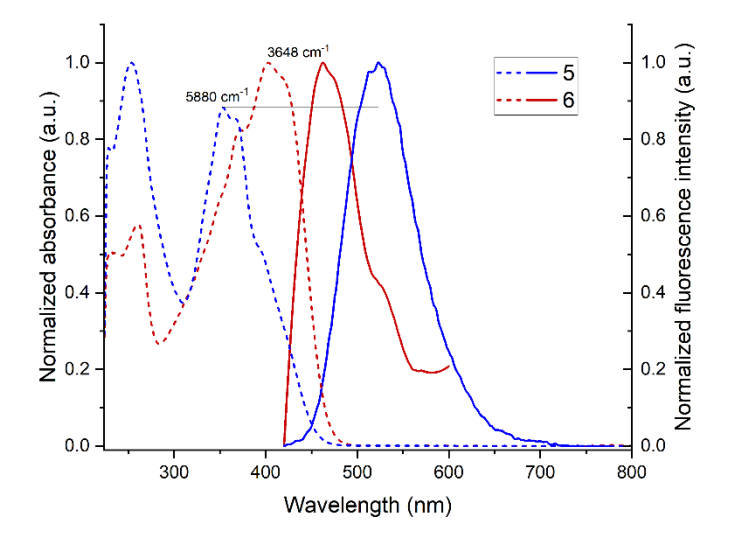


Figure 37. Absorption (dashed line) and emission (straight line) spectra of compounds **5** and **6**.

III.1.2. Metal complexes of diorganoselenium(II) ligands of type R-Se-R

A series of ten metal complexes were obtained by reacting the ligands [4- $\{2-C_6H_5-(4H)-oxazol-5-onă\}C_6H_4\}_2$ Se (5) and [4- $\{2-C_6H_5-(4H)-oxazol-5-onă\}C_6H_4\}_2$ Se (6) with various metal salts: AgOTf, AgPF₆, AuCl(tht) and ZnCl₂. The molar ratio used for the reactions was 1:1 (ligand:metal), as depicted in **Scheme 29**. In addition, a 1:2 molar ratio was used in reaction with AgOTf.

Scheme 29. Synthesis of metal complexes

The ¹H and ¹³C spectra show the resonances corresponding to the expected compounds. Only small differences in the chemical shifts of the resonances, both in the ¹H and the ¹³C{¹H} were observed in the complexes **13-16** when comparing with the ligands **5** and **6**. Comparing the ¹H spectrum of the silver complexes **7-12** no important resonance signal shift can be observed between the AgOTf and AgPF₆ complex in contrast to the 1:1 AgOTf complex with the 1:2 AgOTf complex where we can observe a noticeable shift of the resonance signals corresponding to the protons from the aromatic ring attached to selenium.

In the ⁷⁷Se{¹H} NMR spectra the selenium resonance could be observed only for complexes **13**, **14** and **16** as a singlet in the range 320-443 ppm, corresponding to the typical chemical shift for diorganoselenides, as reported in the literature. ¹²⁸ Comparing the chemical shift of the complexes with the chemical shifts of the ligands we can observe that the values are very similar, indicating that in solution the interactions between the selenium and the metal might not be present as show for similar compounds in literature and instead an nitrogen-metal interaction. ⁶³

The compounds presented a dynamic behavior in solution, at room temperature where the metal atom is being alternatively attached to one of the two organic group as proposed in the literature for the complex [C₆H₄(C₅H₈NO)]₂SeHgCl₂ with a similar structure.¹²⁹ In order to

further support this proposal, a VT NMR study was performed in acetone- d_6 for compound 11. At low temperature two more sets of resonance signals appear. It can be seen more clearly for $H_{12,16}$ and H_7 protons (**Figure 42**). A possible explanation is the splitting of the resonance signals due to formation of two species where the metal is coordinated to one or the other nitrogen as discussed before.

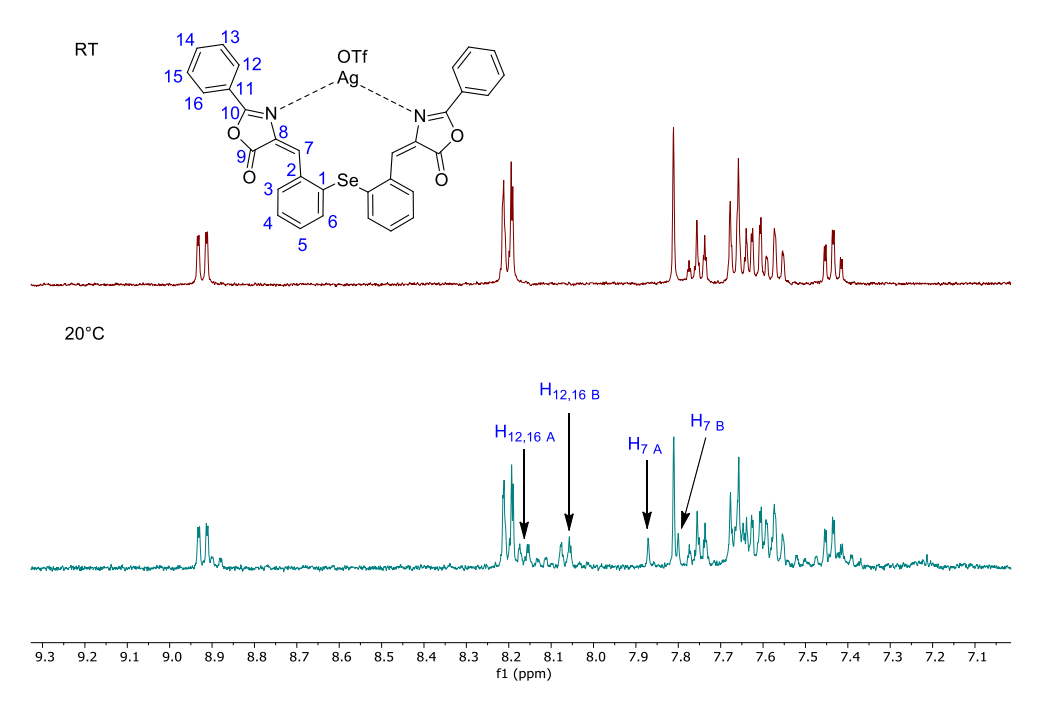


Figure 42. Stacked ¹H NMR spectra of compound **11** at room temperature and after warm up from -50 °C to +20 °C

APCI+ or ESI+ mass spectra were recorded for the complexes **7-16**. In most cases the pseudo-molecular ion could be identified. The [M-OTf]⁺ for complex **8**, [M-PF₆]⁺ for complex **11**, [M-OTf]⁺ for complex **9** and [M-OTf]⁺ for complex **10** peaks could be identified with low intensities (5-10%) and with an intensity of 90-100% in the mass spectrum peaks corresponding to [M-OTf]⁺ for complex **7**, [M-PF₆]⁺ for complex **12** and [M-Cl]⁺ for complex **13**.

The infrared spectroscopy revealed that in complex 7 and 8 the bands corresponding to the oxazolone ring were located in the same region, compared to the ligands 5 and 6. In addition, characteristic bands of the triflate fragment were also observed. The triflate fragment can be identified by the four characteristic bands (asymmetric and symmetric SO₃ and CF₃ stretch). ¹³⁰ In the case of complexes 11 and 12 the band corresponding to the PF₆ was found, based on the literature on MPF₆ compounds, where M is a group I metal. ^{131,132}

Molar conductivity measurements of complexes 7, 8, 11 and 12 were found in the range consistent with 1:1 electrolyte. For complexes 13, 14, 15 and 16 molar conductivity

measurements were found to indicate a non-electrolyte behavior. Complexes 9 and 10 present a molar conductivity in the range consistent with 1:2 electrolytes.¹³³

The crystal structure of compound **9** was determined by single crystal X-ray diffraction. Compound **9** contains two fragments of oxazolone connected through the selenium atom and one dinuclear [Ag₂(OTf)₂] core. The molecule is asymmetric due to the coordination of only one of the oxazolone through the nitrogen atom from the oxazole ring to one of the silver atoms (N1–Ag1 2.266(8) Å; cf. $\Sigma r_{vdW}(Ag,N)^{59}$ 4.25 Å, $\Sigma r_{cov}(Ag,N)$ 2.16 Å⁶⁰). In the crystal structure of compound **9**, four molecules of chloroform are also present as crystallization solvent. The two silver atoms are bridged by the triflate anions, thus generating an eight-membered $Ag_2O_4S_2$ ring through Ag-O bonds of 2.254(7) Å (Ag1-O5), 2.359(6) Å (Ag1-O8), 2.336(6) Å (Ag2-O7) and 2.341(6) Å (Ag2-O10) (cf. $\Sigma r_{vdW}(Ag,O)$ 4.09 Å⁵⁹, $\Sigma r_{cov}(Ag,O)$ 2.11 Å⁶⁰).

Two of the asymmetric units form a dimeric association containing a tetranuclear silver core [Ag₄(OTf)₄] formed by four metal atoms bridged by four triflate moieties. The diorganoselenium fragments act as bridging ligands for the silver atoms through one nitrogen atom (N1–Ag1) and the selenium atom (Ag2–Se1') with a bond length of 2.5691(1) Å (*cf.* $\Sigma r_{vdW}(Ag,Se)$ 4.41 Å⁵⁹, $\Sigma r_{cov}(Ag,Se)$ 2.65 Å⁶⁰) (**Figure 48**).

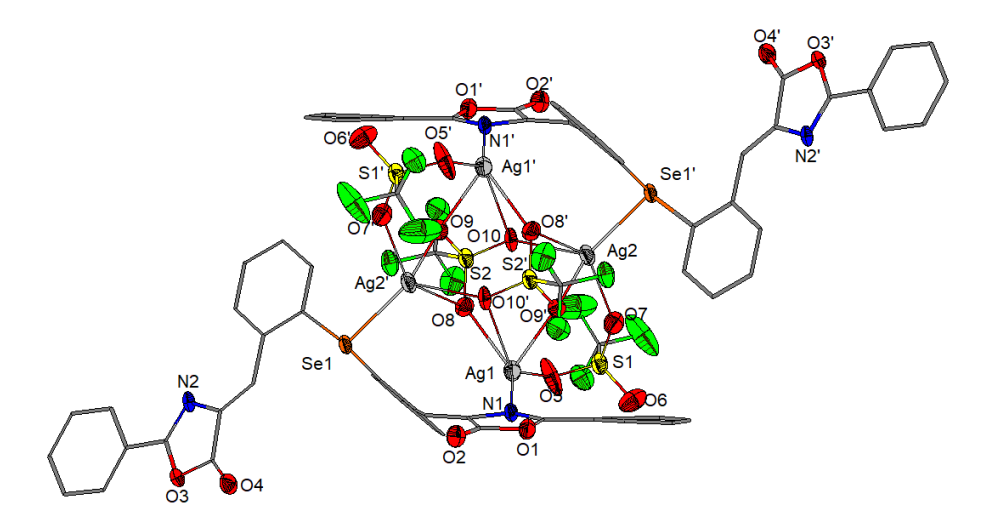


Figure 48. Tetranuclear structure in the crystal of compound **9**. Symmetry equivalent position (2-x, 1-y, 1-z) is given by "prime". Hydrogen atoms and CHCl₃ were omitted for clarity.

In the molecular structure of **9** no Ag···Ag metallophilic interactions were observed. The distances between the silver atoms are 3.959(1) Å for Ag1···Ag2 and 4.345(1) Å for Ag1···Ag2' being longer than the Ag···Ag distance of 3.310 Å observed in similar structures reported in literature, i.e. for [Ag2(OTf)₂(3,3'-DCPA)] (DCPA = dicyanodiphenylacetylene). ¹³⁴

As a result, the two silver atoms are penta-coordinated, thus forming a distorted square-pyramidal coordination geometry, with the τ_5 values of 0.20 and 0.18, respectively.¹³⁵

Intermolecular O···H interactions (H36···O6) of 2.247(9) Å (*cf.* $\Sigma r_{vdW}(O,H)$ 2.70 Å⁵⁹, $\Sigma r_{cov}(O,H)$ 0.97 Å⁶⁰) are formed between the oxygen atom from a triflate anion and a hydrogen atom from a crystallization chloroform molecule, while Cl···H interactions (H32···Cl6') of 2.803(3) Å (*cf.* $\Sigma r_{vdW}(Cl,H)$ 3.02 Å⁵⁹, $\Sigma r_{cov}(Cl,H)$ 1.32 Å⁶⁰), involving an aromatic hydrogen from a phenyl ring and one of the chlorine atoms from the solvent molecule, results in a polymeric chain association in the crystal of **9.** Further more parallel chains are connected by two different interchain F···H contacts (H5···F6'') of 2.487(7) Å (*cf.* $\Sigma r_{vdW}(F,H)$ 2.66 Å⁵⁹, $\Sigma r_{cov}(F,H)$ 0.88 Å⁶⁰), involving a hydrogen atom from the phenyl ring and a fluorine atom from a triflate fragment of a neighboring chain, thus giving rise to a 2D supramolecular network.

In the absorption UV-Vis spectra, the emission maxima were observed for all the compounds in the same region as for the ligand 5 and 6 (Figure 52), except compounds 8 and 14, which did not present fluorescence emission. A hyperchromic shift can be observed in the case complexes 12 and 16 compared to the ligand.

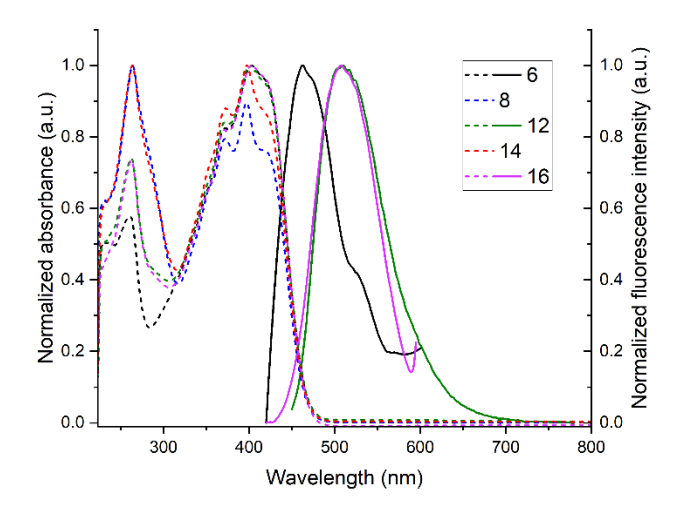


Figure 52. Absorption (dashed line) spectra of compound 6, 8, 12, 14 and 16, and emission (straight line) spectra of compounds 6, 12 and 16.

III.1.3. Diorganoselenium(II) compounds of type R-Se-CH₂-Py-CH₂-Se-R

In **Scheme 31** is presented the reaction pathway for the synthesis of the derivatives based on pyridine functionalized with organoselenium moieties. The diorganodiselenides [(C₃H₃N₂)CH₂CH₂]₂Se₂⁸⁴ (**18**) and (C₆H₄N)₂Se₂⁸⁵ (**19**) have been prepared according to a procedure described in the literature. The new diorganodiselenide [HOC(CH₃)₂CH₂]₂Se₂ (**17**)

and the diorganoselenides {2-[HOC(CH₃)₂CH₂]SeCH₂}₂Py **(20)** [2-(C₅H₄N)SeCH₂]₂Py **(21)** and [2-(C₃H₃N₂)CH₂CH₂SeCH₂]₂Py **(22)** have been prepared by adapted literature methods. The diorganodiselenides were obtained by reacting the corresponding organic halide with Na₂Se₂, previously obtained from sodium borohydride and elemental selenium. The isolated diorganodiselenides were further reacted with sodium borohydride in order to facilitate the cleavage of the Se–Se bond and finally with 2,6-bis(bromomethyl)pyridine to obtain the pure diorganoselenides.

2 R-X + Na₂Se₂ EtOH R-Se-Se-R EtOH NaBH₄ 2 R-SeNa
$$R = R^{1}$$
 (17), R² (18), R³ (19) $R = R^{1}$ (20), R² (21), R³ (22) $R^{1} = R^{1}$ $R^{2} = R^{2}$ $R^{2} = R^{3}$ $R^{3} = R^{3}$ R^{3}

Scheme 31. Synthetic pathway for pyridine derivatives.

NMR spectroscopy was used to identify 18¹³⁶ and 19¹³⁷ which have already been reported in the literature. The resonance signals in the ¹H NMR spectra of compounds 18 and 19 are in agreement with the spectra present in literature. The ¹H NMR spectra of compounds 20, 21 and 22 where found to be similar with spectra of the diorganodiselenides 17, 18 and 19 with the addition of the singlet in the aliphatic region corresponding to the two methylene protons and in the aromatic region the two resonance signals, a triplet and a doublet, corresponding to the H₃ and H₂ protons, respectively, from the pyridine ring were observed, as showed for compound 20 (Figure 53).

In the ⁷⁷Se{¹H} NMR spectra of compounds **18** and **21** a singlet in the range 400-450 ppm, and for compounds **17**, **19**, **20** and **22** a singlet in the range 200-300 ppm were observed, that correspond to the typical chemical shift for diorganodiselenides ¹³⁶⁻¹³⁸ and pyridine based diorganoselenides ⁶⁴⁻⁷⁰, as reported in the literature. Comparing the chemical shift of the diorganodiselenides to diorganoselenides the selenium is shifted upfield with approximately 70 ppm in compound **20** (211 ppm *vs.* 291 ppm), 50 ppm in compound **21** (403 ppm *vs.* 447 ppm) and 50 ppm in compound **22** (238 ppm *vs.* 292 ppm).

In the APCI+ mass spectrum of compound **21** the pseudo-molecular ion $[M+H]^+$ was observed at 421.96695 m/z. In the APCI+ mass spectrum of compound **20**, beside the pseudo-molecular ion $[M+H]^+$ at m/z 412.02954, three other peaks at the m/z values 337.95651,

260.05533 and 185.98199, where the molecule looses one or both arm fragments, as a result of the C-Se bond breaking.

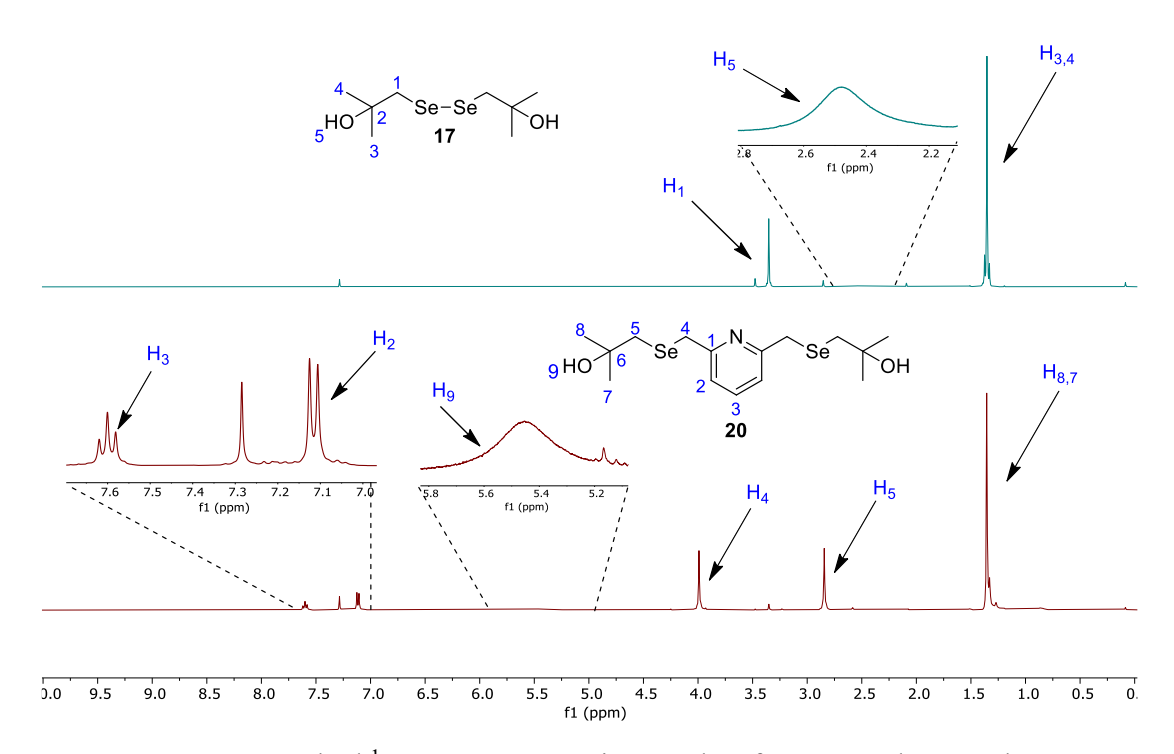


Figure 53. Stacked ¹H NMR spectra, in CDCl₃, of compounds 17 and 20.

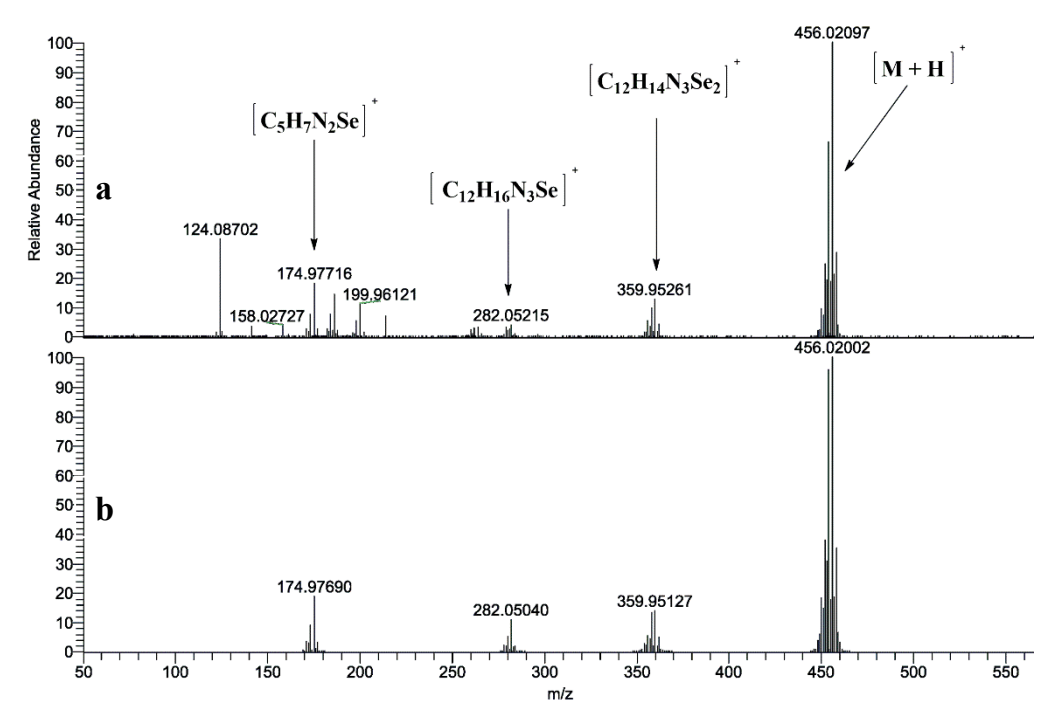


Figure 59. (a) Experimental APCI+ HRMS spectrum of compound **22**, in MeCN, compared with (b) the corresponding simulated peaks.

Similar to the compound **20**, in the APCI+ mass spectrum of compound **22** (**Figure 59**) the pseudo-molecular ion [M+H]⁺ at *m/z* 327.98578 is accompanied by three other peaks at the *m/z* values 359.95261, 282.05215 and 174.97716, the first two corresponding to fragmentation by loosing only one or both arm fragments, as a result of the C–Se bond cleavage, and the third one corresponding to the pyrazole containing arm fragment.

In the structure of compound **20**, one of the two pendant arms is involved in a strong intramolecular N \rightarrow H interaction (H17···N1) of 1.882(1) Å (*cf.* $\Sigma r_{vdW}(N,H)$ 2.86 Å⁵⁹, $\Sigma r_{cov}(N,H)$ 1.02 Å⁶⁰), where the hydrogen from the hydroxyl group interacts with the nitrogen from the pyridine ring. The hydroxyl group from the second pendant arm is involved in a different interaction. O···H interactions of 2.482(4) Å (H4···O3") (*cf.* $\Sigma r_{vdW}(O,H)$ 2.70 Å⁵⁹, $\Sigma r_{cov}(O,H)$ 0.97 Å⁶⁰) between the hydrogen from the methylene group and the oxygen from the hydroxyl group, that lead to a chain-like chain association (**Figure 61**).

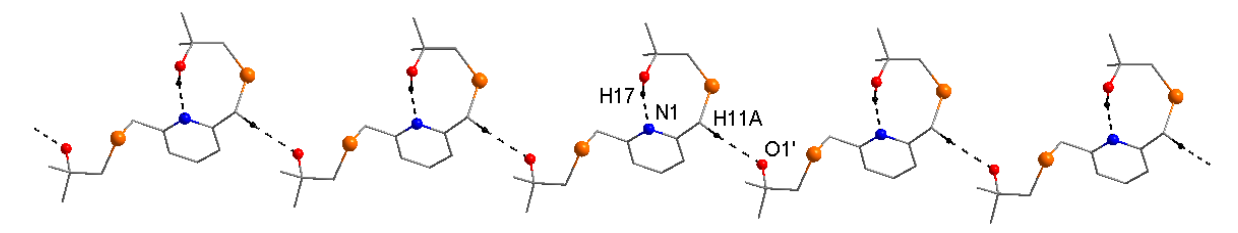


Figure 61. View of a chain in the crystal of compound 20. Hydrogen atoms not involved in intermolecular interactions were omitted for clarity. Symmetry equivalent atoms (x, -1+y, z) are given by "prime".

In compound **21** (**Figure 62**) both selenium atoms have a bent geometry with the bond angles C7–Se1–C6 and C12–Se2–C13 of 100.47(12)° and 99.97(12)°, respectively.

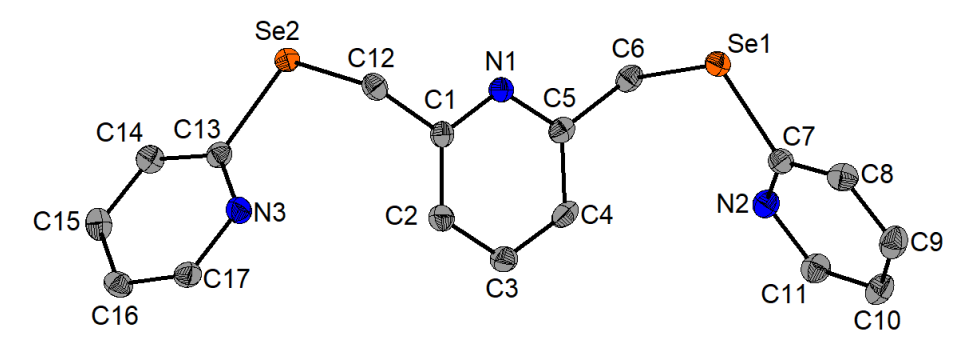


Figure 62. ORTEP-like representation (ellipsoids at 50% probability) of a molecule in compound **21**. Hydrogen atoms were omitted for clarity.

Chains are formed through N···H interactions (H6B···N3') of 2.762(3) Å (*cf.* $\Sigma r_{vdW}(N,H)$ 2.86 Å⁵⁹, $\Sigma r_{cov}(N,H)$ 1.02 Å⁶⁰) between the nitrogen of one of the pyridyl groups and the hydrogen from a methylene group. N···H interactions (H17···N1") of 2.708(2) Å between the nitrogen from the central pyridine ring and the hydrogen from a pyridyl group in a neighbor chain leads to a 2D supramolecular network (**Figure 63**).

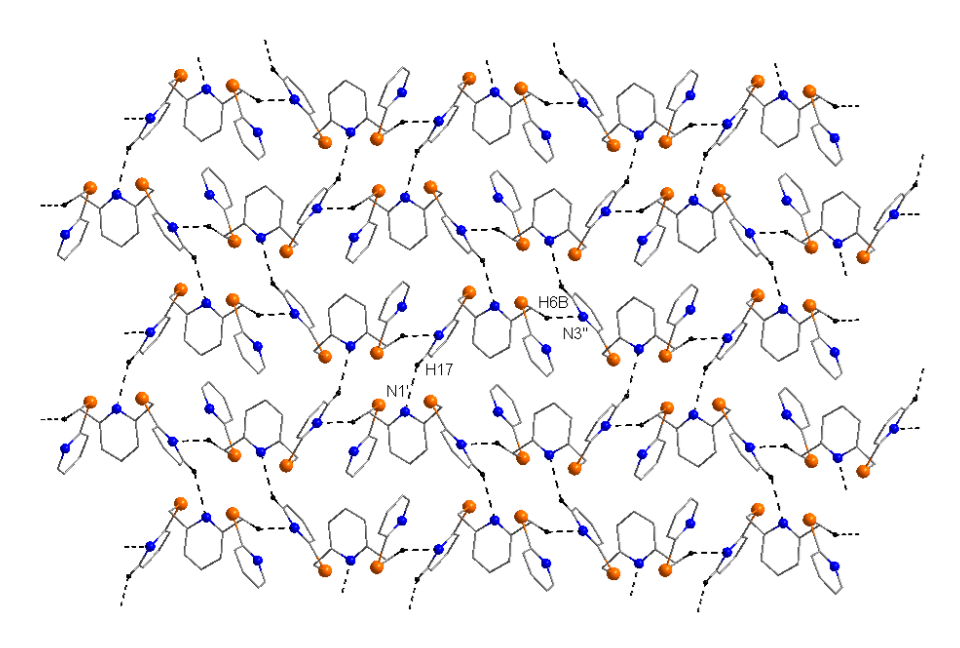


Figure 63. View along axis a of the supramolecular 2D network in the crystal of **21**. Hydrogen atoms that are not involved in intermolecular interactions were omitted for clarity. Symmetry equivalent atoms (1/2-x, 1/2+y, 1/2-z) and (1/2+x, 1/2-y, 1/2+z) are given by "prime" and "double prime", respectively.

The UV-Vis spectra of compounds **20** and **22** showed a band in the range 250-325 nm while in compound **21** it showed a band in the range 200-275 nm.

III.1.4. Metal complexes of diorganoselenium(II) ligands of type R-Se-CH₂-Py-CH₂-Se-R

A series of metal complexes were obtained by reacting the neutral ligands {2-[HOC(CH₃)₂CH₂]SeCH₂}₂Py (20), [2-(C₅H₄N)SeCH₂]₂Py (21) and [2-(C₃H₃N₂)CH₂CH₂SeCH₂]₂Py (22) with various metal salts (Scheme 32). The chemical reactivity of the ligands was investigated towards AgOTf, AgPF₆, AgNO₃, AuCl(tht), AuC₆F₅(tht) and Cul. In the case of gold complexation, all three ligands were not suitable and no pure compounds were isolated due to fast decomposition.

$$R = R^{1} (20, L^{1}), R^{2} (21, L^{2}), R^{3} (22, L^{3})$$

$$R = R^{1} (20, L^{1}), R^{2} (21, L^{2}), R^{3} (22, L^{3})$$

$$R = R^{1} (20, L^{1}), R^{2} (21, L^{2}), R^{3} (22, L^{3})$$

$$R = R^{1} (20, L^{1}), R^{2} (21, L^{2}), R^{3} (22, L^{3})$$

$$R^{2} = R^{1} (20, L^{1}), R^{2} (21, L^{2}), R^{3} (22, L^{3})$$

$$R^{3} = R^{1} (20, L^{1}), L^{2} (21, L^{2}), R^{3} (21, L^{2})$$

$$R^{3} = R^{1} (20, L^{1}), L^{2} (21, L^{2}), R^{3} (21, L^{2})$$

Scheme 32. Synthesis of group 11 metal complexes.

The ¹H and ¹³C NMR spectra show the resonances corresponding to the expected compounds and the ¹⁹F and ³¹P NMR indicate that there is only a single species present.

The ¹H NMR spectrum of complex **23** suggests that the pyridine nitrogen coordinates to the silver, thus influencing the overall chemical environment. The ⁷⁷Se NMR spectrum suggests the coordination of selenium also, due to the shift of the resonance from approximately 210 to 190 ppm.

In the ¹H NMR spectrum of the complexes of ligands 21 and 22 there is no change in multiplicity or the number of resonance signals, meaning that the two pendant arms are equivalent in solution. Comparing the silver complexes noticeable differences are observed between compounds 24 and 26, as compared to the compounds 25 and 27 where only small chemical shifts is present. The ⁷⁷Se NMR spectrum of complex 25, 27 and 29 confirms the coordination of selenium to the metal due to the shift from approximately 240 to 215 ppm. Only one resonance signal is present in each case which confirms that in solution the metal undergoes a dynamic behavior, or it's attached to both selenium. This trend could be the case in all complexes, including those of ligand 21.

In the ESI+ mass spectra of the metal complexes of ligands **20**, **21** and **22** in all of the cases the base peak corresponds to the cation [M-OTf]⁺, [M-PF₆]⁺, [M-NO₃]⁺ or [M-I]⁺ was found. For all the complexes, except for compound **29**, the second most intense peak corresponds to a fragment of the base peak where it loses a pendant arm. The break takes place at one C–Se bond and the lost fragment is [HOC(CH₃)₂CH₂]Se, (C₅H₄N)Se or (C₃H₃N₂)CH₂CH₂Se depending on the ligand.

Molar conductivity measurements of complexes 23, 24, 25, 26, 27 and 29 were found in the range or very close to the range consistent with 1:1 electrolytes. For the CuI complexes 30 and 31 molar conductivity measurements indicated a non-electrolyte behavior. 130

In the solid state structure of compound 24 the molecule is asymmetric due to the coordination of only one pendant arm through the nitrogen atom from a pyridyl fragment to the

silver atom (Ag1–N3 2.214(1) Å; cf. $\Sigma r_{vdw}(Ag,N)^{59}$ 4.25 Å, $\Sigma r_{cov}(Ag,N)$ 2.16 Å⁶⁰). The molecules are associated in dimeric units (**Figure 73**). The ligand acts as a bridging unit, interacting with the silver atoms through two of the nitrogen atoms, one nitrogen from the central pyridine ring (Ag1–N1') with a length of 2.333(1) Å, and the other from the pyridyl group in one pendant arm (N3–Ag1), as well as by the two selenium atoms (Ag1–Se1' 3.510(3) Å and Ag1–Se2' 2.654(4) Å, cf. $\Sigma r_{vdw}(Ag,Se)$ 4.41 Å⁵⁹, $\Sigma r_{cov}(Ag,Se)$ 2.65 Å⁶⁰).

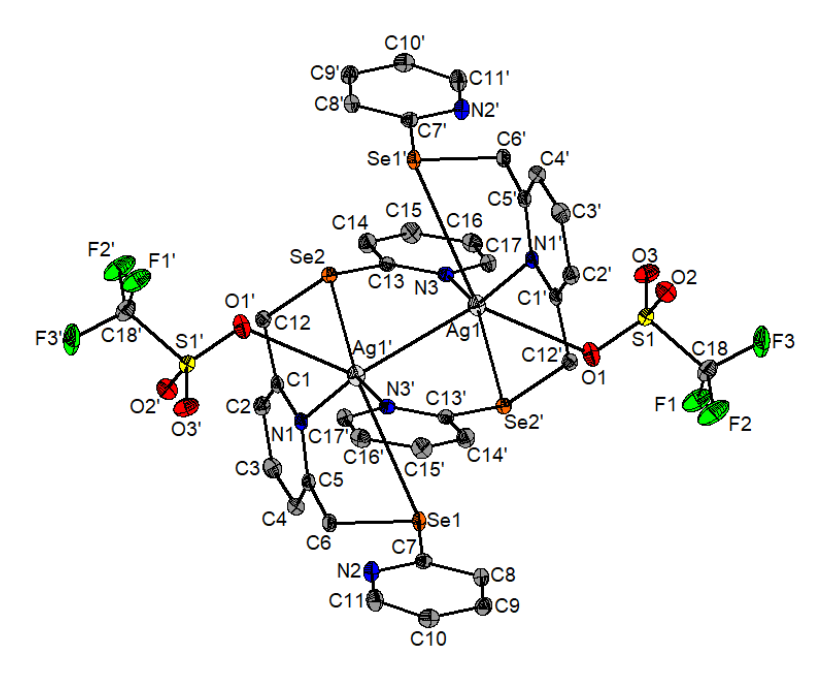


Figure 73. Dimeric association in the crystal of compound **24**. Symmetry equivalent position (1-x, 1-y, 1-z) is given by "prime". Hydrogen atoms were omitted for clarity.

The silver atoms are hexa-coordinated with a Ag···Ag metallophilic interaction. The distance between the silver atoms of 3.094(4) Å is in the range of 2.9 - 3.3 Å similar to the Ag···Ag intermolecular interaction of 3.250(4) Å, 2.909(6) Å and 2.911(6) Å found in the hexa-coordinated pseudo-polymorph dimers $[Ag_2(tpp)_2][BF_4]_2$ ·MeNO₂ [tpp = 2,4,6-tri(pyrazol-1-yl)pyridine]. 139

The $Ag_2N_3OSe_2$ coordination sphere can be described as being constituted of two triangle planes (O1, N1', Se2' and N3, Se1', Ag1') and the geometry around the silver in compound 24 can be regarded as a distorted trigonal prism as observed also in compound $[Ag_4(hfac)_4(\mu_2-bpm)_3]$ (hfac = 1,1,1,5,5,5-hexafluoroacetylacetonate, bpm = 2,2'-bipyrimidine).¹⁴¹

Intermolecular O···H interactions (H6A···O2" and H4···O3") of 2.464(1) Å and 2.428(1) Å (*cf.* $\Sigma r_{vdW}(O,H)$ 2.70 Å⁵⁹, $\Sigma r_{cov}(O,H)$ 0.97 Å⁶⁰) are formed between the oxygen atoms

from a triflate anion and hydrogen atoms from the methylene group and the pyridyl ring, respectively, thus resulting in a chain-like association in the crystal of **24** (**Figure 75**).

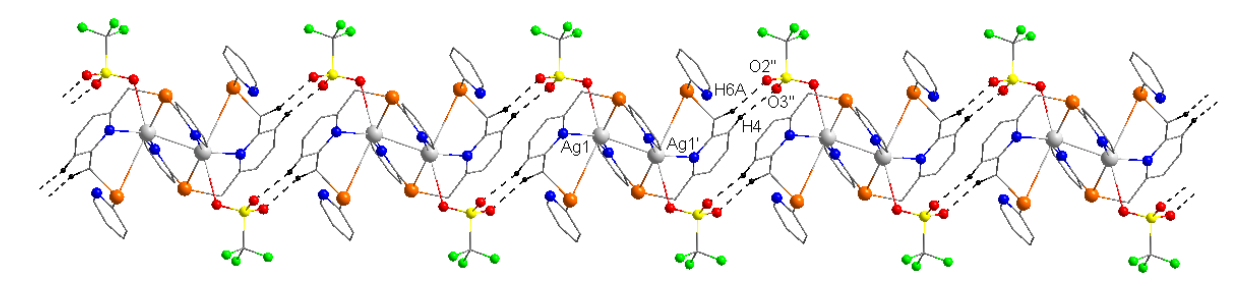


Figure 75. Chain-like association in the crystal of **24**. Hydrogen atoms that are not involved in intermolecular interactions were omitted for clarity. Symmetry equivalent atoms (1-x, 1-y, 1-z) and (-1+x, y, z) are given by "prime" and "double prime", respectively.

The structure of compound **25** is asymmetric as well. Like in the compound **23** only one of the pendant arm is coordinated to silver, through selenium (Ag1–Se2 2.958(3) Å; *cf.* $\Sigma r_{vdW}(Ag,Se)$ 4.41 Å⁵⁹, $\Sigma r_{cov}(Ag,Se)$ 2.65 Å⁶⁰) and one nitrogen atom from the pyrazole fragment (Ag1–N5 2.271(2) Å; *cf.* $\Sigma r_{vdW}(Ag,N)^{59}$ 4.25 Å, $\Sigma r_{cov}(Ag,N)$ 2.16 Å⁶⁰).

Each selenium and nitrogen from the pyridine ring are involved in interaction with the silver from the neighboring molecule (Ag1'–Se2 3.2498(3) Å; Ag1'–Se1 2.733(4) Å; Ag1'–N1 2.320(2) Å), thus resulting in a coordination polymer (**Figure 78**). The geometry around the silver atom is a distorted square pyramid with the nitrogen from the pyridine in apices, confirmed by $\tau_5 = 0.2$ ($\tau = 0$ for an ideal square pyramid and $\tau = 1$ for an ideal trigonal bipyramid).¹³⁵

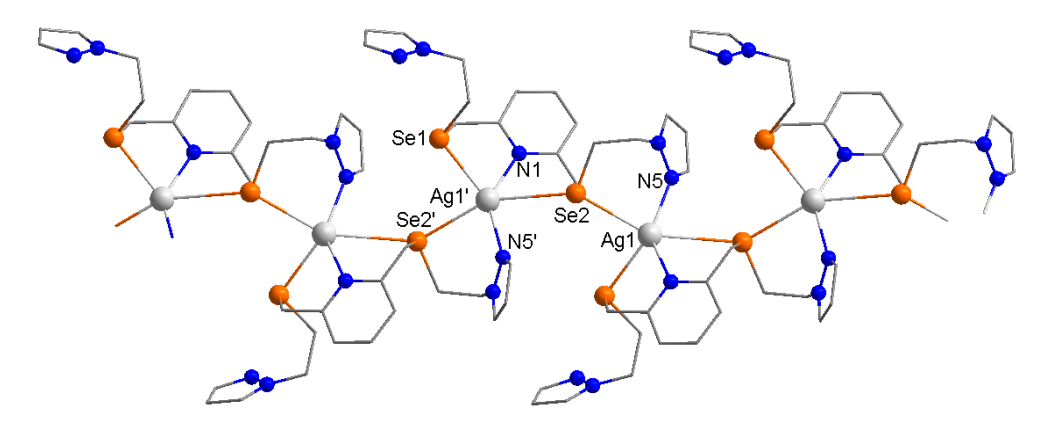


Figure 78. Polymeric chain in the crystal of **25**. Hydrogen atoms that are not involved in intermolecular interactions were omitted for clarity. Symmetry equivalent atoms (3/2-x, -1/2+y, 1/2-z) are given by "prime".

The molecular structure of compound **27** is very similar to that of compound **25**, except the different anion. The same coordination pattern can be observed, where only one of the pendant arm coordinates to silver through the selenium (Ag1–Se1 2.901(4) Å; *cf.* $\Sigma r_{vdw}(Ag,Se)$ 4.41 Å⁵⁹, $\Sigma r_{cov}(Ag,Se)$ 2.65 Å⁶⁰) and one nitrogen atom from the pyrazole fragment (Ag1–N3 2.271(2) Å; *cf.* $\Sigma r_{vdw}(Ag,N)^{59}$ 4.25 Å, $\Sigma r_{cov}(Ag,N)$ 2.16 Å⁶⁰). Like in compound **25**, each selenium and the nitrogen from the pyridine ring are involved in interactions with the silver from the neighboring molecule (Ag1'–Se1 3.322(4) Å; Ag1'–Se2 2.781(4) Å; Ag1'–N1 2.301(2) Å) to form a coordination polymer. The length of these interactions are almost the same as in compound **25**, and likewise the resulting geometry is distorted square pyramid with the geometry index being slightly bigger $\tau_5 = 0.3$ ($\tau = 0$ for an ideal square pyramid and $\tau = 1$ for an ideal trigonal bipyramid).¹³⁵

In the molecular structure of compound **30** (**Figure 84**) a strong coordination to the metal of only one of the selenium from one of the pendant arm (Cu1–Se1 2.466(2) Å; *cf.* $\Sigma r_{vdW}(Cu,Se)$ 4.20 Å⁵⁹, $\Sigma r_{cov}(Cu,Se)$ 2.52 Å⁶⁰) and only one of the nitrogen from the other pendant arm (Cu1–N3 2.021(13) Å; *cf.* $\Sigma r_{vdW}(Cu,N)^{59}$ 4.04 Å, $\Sigma r_{cov}(Cu,N)$ 2.03 Å⁶⁰) are observed. The nitrogen from the central pyridine is also coordinated to the copper atom (Cu1–N1 2.042(1) Å). The resulting geometry around the copper center is a trigonal pyramid.

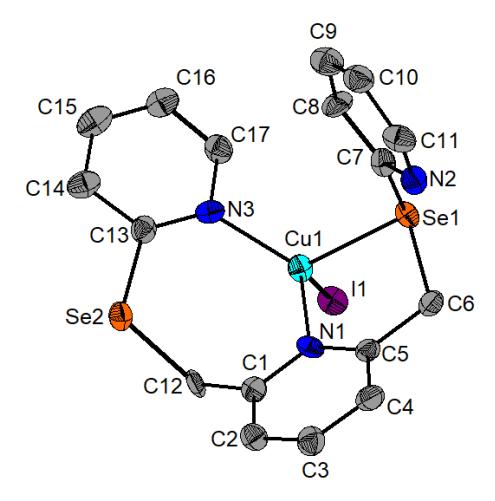


Figure 84. ORTEP-like representation (50% probability ellipsoids) in compound **30**. Hydrogen atoms were omitted for clarity.

The second selenium forms a weak I···Se contact of 3.760(2) Å (I1···Se2") (*cf.* $\Sigma r_{vdW}(I,Se)$ 3.86 Å⁵⁹, $\Sigma r_{cov}(I,Se)$ 2.59 Å⁶⁰) with iodine. The long chains formed are further connected by weak I···H interaction of 3.071(1) Å (I1····H8) (*cf.* $\Sigma r_{vdW}(I,H)$ 3.24 Å⁵⁹, $\Sigma r_{cov}(I,H)$ 1.70 Å⁶⁰) resulting in a 2D network (**Figure 85**).

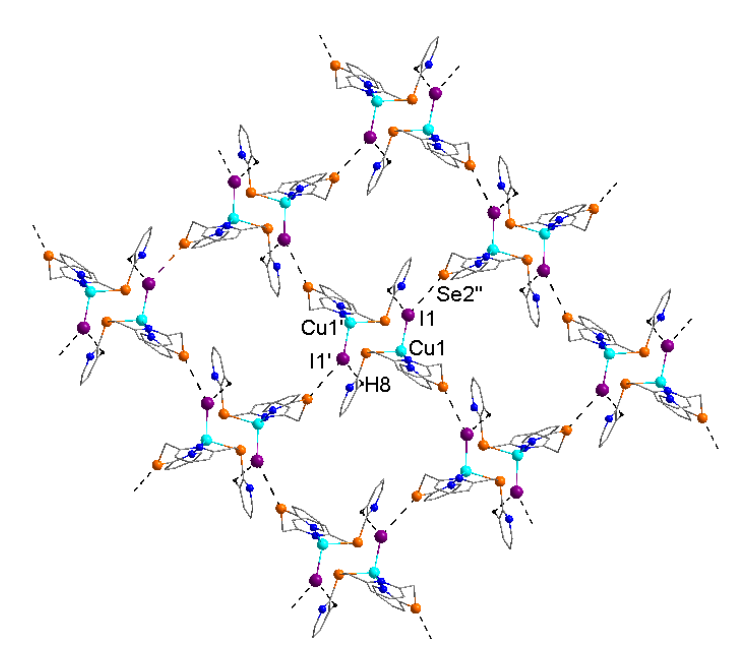


Figure 85. Best view of the supramolecular 2D network in the crystal of **30**. Hydrogen atoms that are not involved in intermolecular interactions were omitted for clarity. Symmetry equivalent atoms (1–x, 1–y, 1–z) and (1/2+x, 1/2-y, -1/2+z) are given by "prime" and "double prime", respectively.

In the UV-Vis spectra compound 23 as compared with ligand 20 shows a decrease in intensity for the band corresponding to the intra-ligand transitions in the range of 270 nm and also an increase in the range of 320-400 nm corresponding to the metal-ligand transitions. The same trend is also present for the compounds 25, 27, 29, 26 and 30. Compound 31 presents a large band at 250 nm while compound 24 at 270 nm when compared with their ligand. The most notable change in the visible region is for the copper complexes where a new broad band is present (Figure 87).

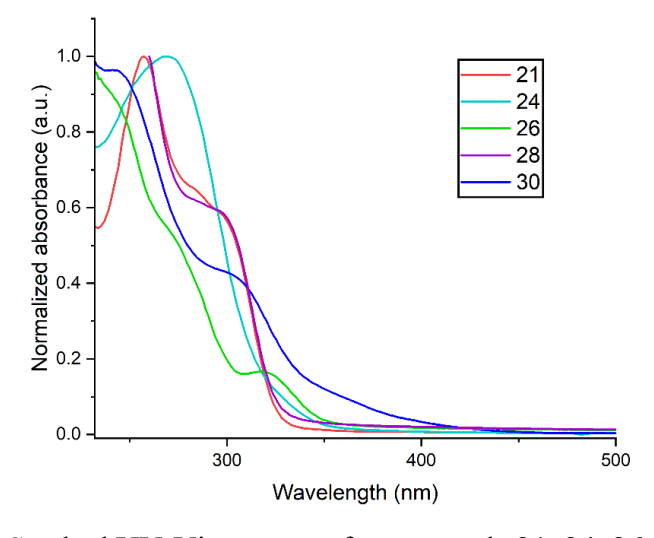


Figure 87. Stacked UV-Vis spectra of compounds 21, 24, 26, 28 and 30.

III.2. Imidazolone and thiazolone compounds

III.2.1. Imidazolones and thiazolones

In this subchapter a series of thiazolones and imidazolones containing one or two substituents located at the 4-arylidene ring were synthesized. The photophysical properties of the compounds can be controlled by the effect of the electron density. By that reason the substituents were chosen as either electron-withdrawing groups such as fluorine or chlorine or electron-donating groups such as methoxy. The positions of the substituents on the arylidene ring (position 4, positions 3 and 4 and positions 2 and 4) were selected to control the steric hindrance. The *n*-propyl group was chosen as substituent for the nitrogen from the imidazolone ring because of its chemical inertness and for the further aid in the ¹H NMR investigations.

The synthesis of imidazolones 4-(4-fluorobenzylidene)-2-phenyl-5(4*H*)-imidazolone (37), 4-(4-chlorobenzylidene)-2-phenyl-5(4*H*)-imidazolone (39), 4-(3,4-metoxybenzylidene)-2-phenyl-5(4*H*)-imidazolone (40) and 4-(2,4-metoxybenzylidene)-2-phenyl-5(4*H*)-imidazolone (41) have been prepared by following the procedure described in the literature. The thiazolones 4-(4-fluorobenzylidene)-2-phenyl-5(4*H*)-thiazolone (42), 4-(4-chlorobenzylidene)-2-phenyl-5(4*H*)-thiazolone (43), 4-(3,4-metoxybenzylidene)-2-phenyl-5(4*H*)-thiazolone (45) and 4-(2,4-metoxybenzylidene)-2-phenyl-5(4*H*)-thiazolone (46) have been prepared according to the literature. 144

The methods of synthesis involve directly converting the corresponding oxazolone into thiazolones or imidazolones. The oxazolones were synthesized according to the standard Erlenmeyer-Plöchl procedure, by reacting the corresponding hippuric acids and aldehyde in acetic anhydride (**Scheme 33**). 125

$$R = 4-F (32), 4-Cl (33), 3, 4-Cl (34)$$

R = 4-F (32), 4-Cl (33), 3,4-Cl (34), 3,4-MeO (35), 2,4-MeO (36)

Scheme 33. Synthesis of oxazolones.

The oxazolones 4-(4-fluorobenzylidene)-2-phenyl-5(4H)-oxazolone (32), ¹⁴⁵ 4-(4-chlorobenzylidene)-2-phenyl-5(4H)-oxazolone (33), ¹⁴⁶ 4-(3,4-chlorobenzylidene)-2-phenyl-5(4H)-oxazolone (34), ¹⁴⁷ 4-(3,4-metoxybenzylidene)-2-phenyl-5(4H)-oxazolone (35) ¹⁴⁸ and 4-

(2,4-metoxybenzylidene)-2-phenyl-5(4H)-oxazolone $(36)^{149}$ were synthesized previously with the same method.

The imidazolones were obtained by reacting the previously obtained oxazolones with *n*-propylamine in pyridine and N,O-bistrimethylsilylacetamide (BSA) as promoter (**Scheme 34**).

Scheme 34. Synthesis of imidazolones.

The thiazolones were obtained by reacting the previously obtained oxazolones with thioacetic acid and trimethylamine (**Scheme 35**).

$$R = 4-F (32), 4-Cl (33), 3,4-Cl (34), 3,4-MeO (35), 2,4-MeO (36)$$

$$R = 4-F (42), 4-Cl (43), 3,4-Cl (44), 3,4-MeO (45), 2,4-MeO (46)$$

Scheme 35. Synthesis of thiazolones.

In the stacked ¹H NMR spectra of the compounds substituted in the para position of the arylidene ring, compounds **37** and **38** (**Figure 88**), one set of the resonance signals was observed. In the aliphatic region two triplets and one quartet were observed for the propyl group. In the aromatic region the resonance signal from the methine proton appears as a singlet, while the protons in the two aromatic rings give multiplet resonances. In both aromatic groups the ortho as well as the meta protons are equivalent. In the case of compound **37** the resonance signals from the arylidene ring are split due to the F-H coupling. This is also confirmed by the ¹³C (APT) NMR of compound **37**, where the splitting of the resonance signals can be seen even at the methine carbon.

In the ¹H NMR spectra of the compounds **39**, **40** and **41** beside the resonance signals corresponding to the phenyl and the propyl groups, also present in the compound **37** and **38**, there are three other resonance signals corresponding to the protons from the arylidene, and the ortho and meta protons are no longer equivalent. For the compounds **40** and **41** another two

singlets corresponding to the methoxy groups can be observed in the aliphatic region. Comparing the two methoxy substituted compounds, the H_{16} proton from the ortho position of the arylidene, where the ortho palladation will occur, is shifted downfield with over 1 ppm in compound 41 as compared to 40. The change in chemical shift may give insight on the influence of the position of the substituents on the arylidene ring and as consequence on the electron density.

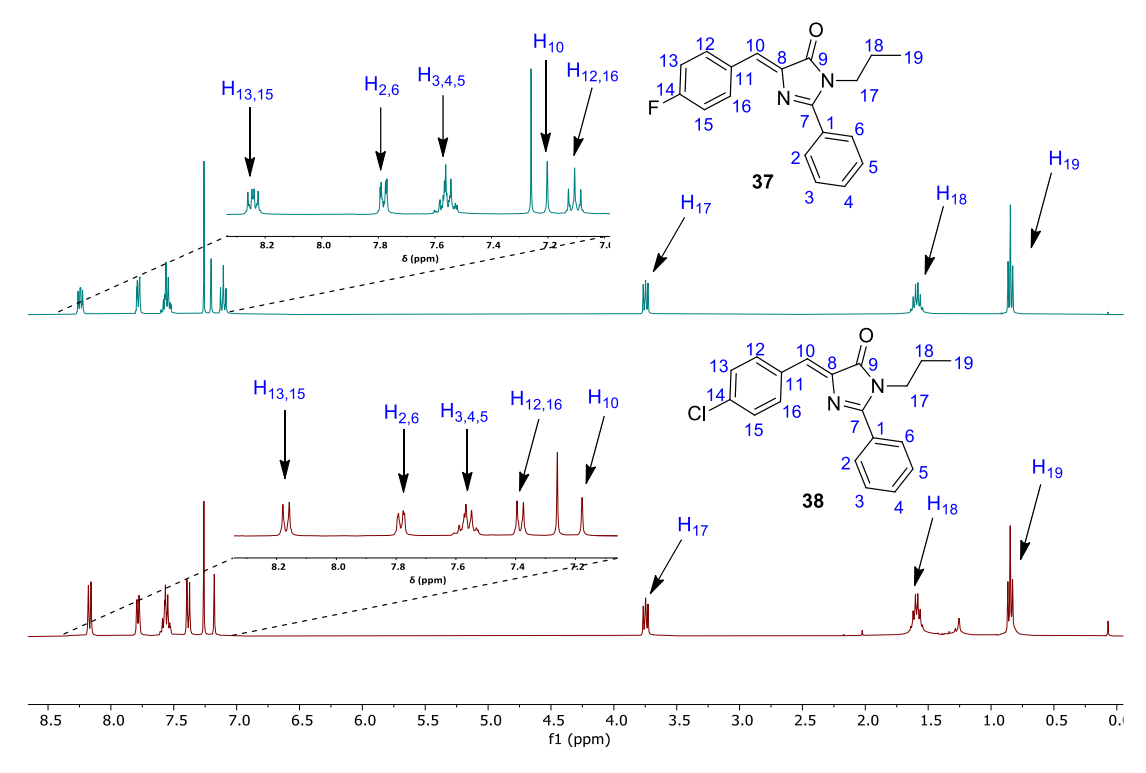


Figure 88. Stacked ¹H NMR spectra of compounds 37 and 38.

In the ESI+ mass spectrum of the imidazolones the pseudo-molecular ion [M+H]⁺ of compounds **37** (m/z 309.1405), **38** (m/z 325.1100), **39** (m/z 359.0730), **40** (m/z 351.1689) and **41** (m/z 351.1705) appears with an intensity between 5% and 50%. The [M+Na]⁺ ion is present in all spectra: compound **37** (m/z 331.1226), **38** (m/z 347.0928), **39** (m/z 381.0538), **40** (m/z 373.1522) and **41** (m/z 373.1519), and in case of compounds **37**, **38** and **40** these cations represent the base peak.

III.2.2. Orthopalladated imidazolones and thiazolones

Orthopalladated complexes of thiazolones and imidazolones were synthesized by reactions with palladium acetate, in trifluoroacetic acid (**Scheme 36**). The final products were dimers bridged by trifluoroacetato ligands. The orthopalladation reaction of thiazolone **46** failed, even if several different reaction conditions were attempted (temperatures, reaction times or solvents were changed).

Scheme 36. Synthesis of orthopalladated products.

$$Z = N^{n}Pr$$

$$R = 4-F (47), 4-Cl (48), 3,4-Cl (49)$$

$$Z = S$$

$$R = 4-Cl (53), 3,4-Cl (54)$$

$$Z = N^{n}Pr$$

$$R = 4-F (56), 4-Cl (57), 3,4-Cl (58)$$

$$Z = S$$

$$R = 4-Cl (59), 3,4-Cl (60)$$

Scheme 37. Synthesis of the [2+2]-cycloaddition products.

The [2+2]-cycloaddition of the orthopalladated products was achieved by irradiation with blue light (Scheme 37). The compounds presented very different photochemical properties: compound 50, 51 and 55 did not undergo cycloaddition, irradiation of compound 52 resulted in a mixture of isomers that could not be separated and irradiation of compounds 47, 48, 49, 53 and 54 lead to the selective formation of the corresponding cyclobutanes, namely only one diastereoisomer, the ε-isomer.

In order to further understand and improve the fluorescence of the synthesized orthopalladated compounds a change of the ancillary ligands was employed by following the appropriate literature. ¹⁵⁷⁻¹⁶⁰ Imidazolone **51** was used in further reactions involving an exchange of ligand.

As shown in **Scheme 38** the dinuclear derivative **51** was either reacted with pyridine in 1:2 molar ratio to yield the mononuclear derivative **61** or treated with LiCl in 1:4 molar ratio in

MeOH to obtain the dinuclear chloride bridged complex **62**. Complex **62** was subsequently reacted with pyridine in 1:2 molar ratio in CH₂Cl₂ to form the mononuclear complex **63**, with Tl(acac) in 1:2 molar ratio in CH₂Cl₂ (acac = acetylacetonate) to afford the neutral mononuclear complex **64**, and with AgBF₄ and pyridine in a 1:2:4 molar ratio, in CH₂Cl₂ and acetone, respectively, to give the cationic bis-pyridine derivative **65**.

Scheme 38. Synthesis of the fluorescent imidazolone derivatives 61, 62, 63, 64 and 65.

All ¹H NMR spectra of the orthopalladation products show no resonance signals for H₁₆ proton which confirms that the C-H bond activation took place. Additionally, the overall resonance signals corresponding to the arylidene ring changed, this includes the multiplicity, chemical shift, and the number of signals of the para substituted compounds as the protons are no longer equivalent.

For example, by comparing compound **48** with its precursor, compound **38**, in the stacked ¹H NMR spectra (**Figure 92**), in the aromatic region we can observe a change in the number of resonance signals corresponding to the arylidene. In the aliphatic region of compound **48** the resonance signals from the methylene groups in the propyl fragment present a diastereotopic character which support that the C–H bond activation occurred. This result is due to the relative anti arrangement of the orthopalladated moieties in the dimer. In the HSQC spectrum we can see that both multiples are coupled to the same carbon resonance.

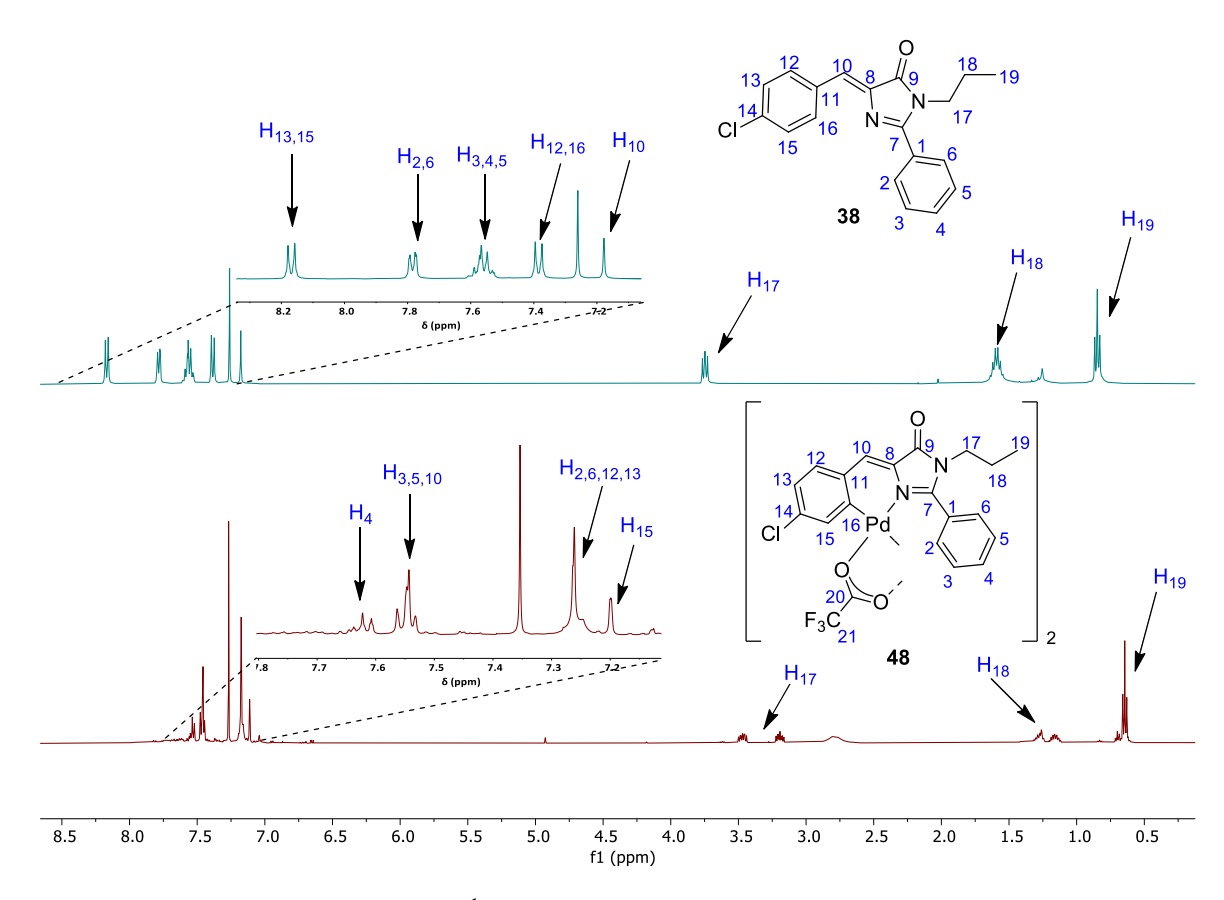


Figure 92. Stacked ¹H NMR spectra of compounds 38 and 48.

If we compare the NMR of the [2+2]-cycloaddition products with the orthopalladated dimers we should observe a shift of the resonance of the protons from the methine group, as a new bond is formed. This is indeed true, as shown for compound 57, where the resonance corresponding to the H₁₀ proton shifts from approximately 7 ppm to approximately 5 ppm. In the stacked ¹H NMR spectra of compounds 48 and 57 (Figure 94) this shift is evident and as a result of the formation of the cycle the resonance signals corresponding to the arylidene moiety are also shifted due to the change in the overall chemical environment.

In addition, in the 13 C NMR spectrum the resonance signals corresponding to the carbons present in the methine group, C_8 and C_{10} , are considerably shifted. For example, in the 13 C NMR spectra of compounds **49** and **58** the C_8 carbon shifts from approximately 133 ppm to approximately 70 ppm and the C_{10} shifts from approximately 133 ppm to approximately 58 ppm.

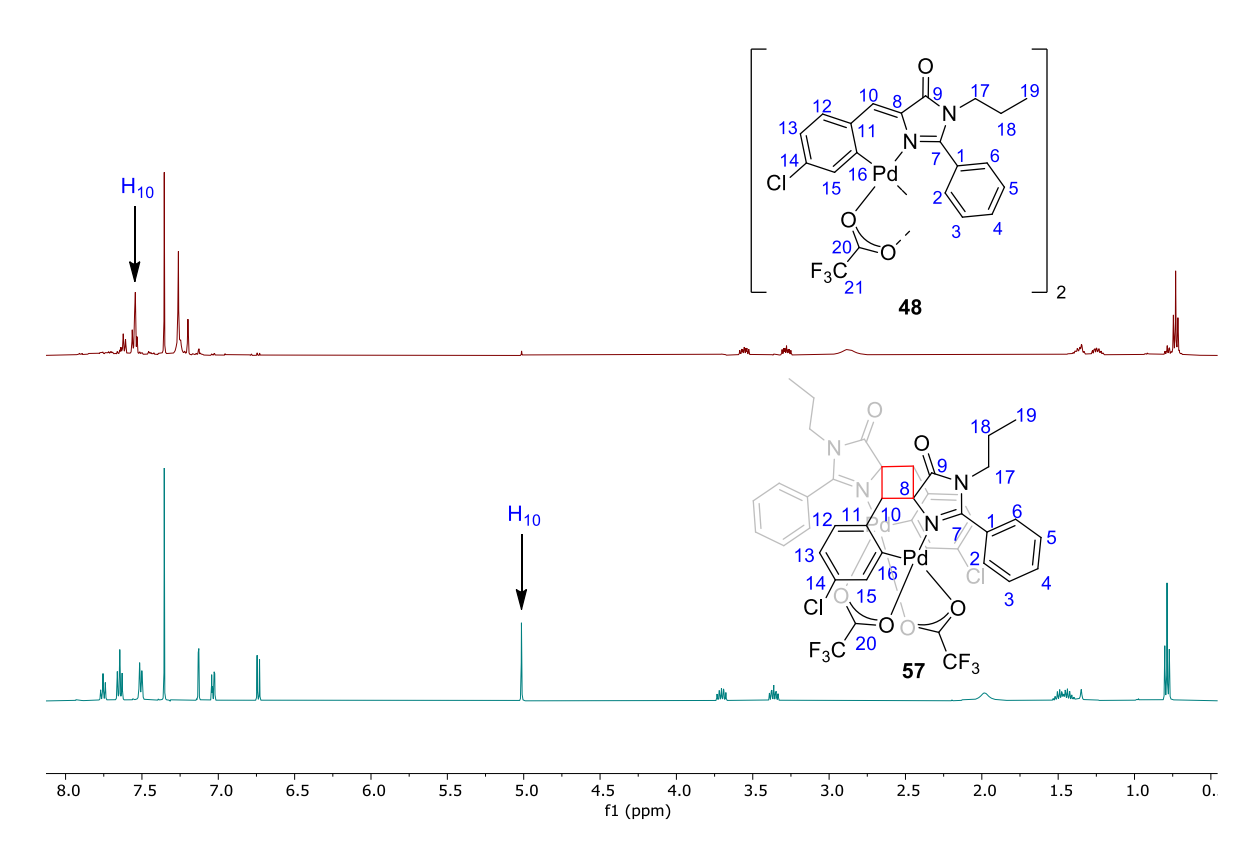


Figure 94. Stacked ¹H NMR spectra of compounds 48 and 57.

Complexes **61**, **63**, and **65** exhibit a dynamic behavior in solution at room temperature. By lowering the temperature to 233 K the molecules become static during the response time of the NMR. **Figure 98** shows the stacked ¹H NMR spectra of the ligand **51** and the complexes **61** and **63**. Both compounds present *cis* and *trans* isomer mixtures, in 1:1 ratio in case of compound **63** and in 1:4 ratio in the case of compound **61**. Consequently, in the ¹H NMR spectra two sets of resonance signals can be observed, more clearly seen in the aliphatic region at the protons from the propyl group and the two methoxy groups. The spectra show also that there is no longer a dimer and instead a monomeric compound is formed, indicated by the H₁₉ and H₂₀ protons which no longer have a diastereotopic character.

In the ¹H NMR spectrum of the complex **64**, in the aliphatic region the resonance signals from the the propyl group indicate that the monomer is formed. The resonance signals of the H₂₃, H₂₄ and H₂₆ protons correspond to the acetylacetonate group in which the two methyl fragments are nonequivalent.

In the ¹H NMR spectrum of the complex **65** in the aromatic region there are two additional sets corresponding to two pyridine groups in addition to the resonance signals also present in the compound **51**. This is evident by the two most deshielded resonance signals, which are not overlapping, corresponding to the protons in the *ortho* position of the pyridine. It

is also supported by the single set of resonance signals in the aliphatic region which indicates that all the resonance signals correspond to the only one monomeric species.

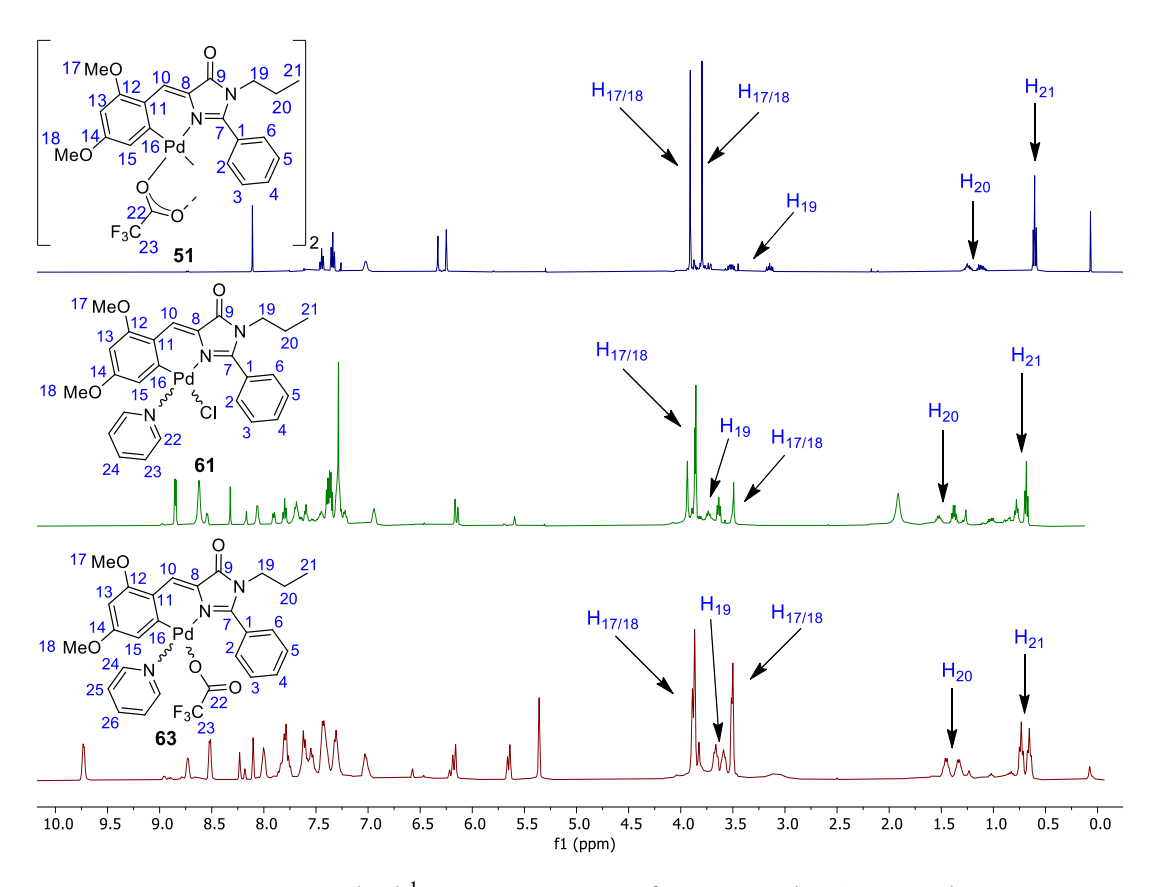


Figure 98. Stacked ¹H NMR spectra of compounds 51, 61 and 63.

In the ESI+ mass spectrum of the orthopalladated compounds no [M+H]⁺ ion was found. The [M+Na]⁺ ion was observed in case of imidazolone derivatives **47** (m/z 1077.0201), **49** (m/z 1178.8733), **50** (m/z 1161.0782) and **51** (m/z 1161.0736) and thiazolone derivatives **53** (m/z 1158.7848) and **55** (m/z 1110.9030) with low intensity (5%-10%). Other ions such as [M-CF₃CO₂]⁺, representing the base peak in case of the imidazolone derivatives **47** (m/z 941.0460), m/z **48** (972.9930), **49** (m/z 1042.8987), **50** (m/z 1025.1060) and **51** (m/z 1025.1034) and thiazolone derivatives **52** (m/z 890.8809) and [M-2CF₃CO₂-H]⁺ in **54** (m/z 878.7758). In the ESI+ mass spectrum of the orthopalladated compounds with various ancillary ligands the molecular ion [M]⁺ or the pseudo molecular ion [M+H]⁺ were observed for **61** (m/z 646.0801), **62** (m/z 980.0567) and **65** (m/z 555.1112), respectively. In the spectra of **63** and **64** the peaks for the cations [M-Cl+H]⁺ (m/z 534.1004) and [M-2py]⁺ (m/z 455.0606), respectively, were found.

The solid state structures of the thiazolones **52** and **53** and the imidazolone **49** (**Figure 102**) were determined by single-crystal X-ray diffraction. The compounds adopt an open-book structure. Although the palladium atoms are close each other no metal-metal interaction is observed. The palladium is bonded covalently with four other atoms: with nitrogen (2.0152(14) in **52**, 2.0339(15) in **53** and 2.0170(13) in **49**, *cf.* Σr_{cov}(Pd,N) 2.10 Å⁶⁰), with the oxygen from each trifluoro acetate ligand (2.1759(14) and 2.0418(12) in **52**, 2.1639(14) and 2.0535(14) in **53**, 2.1622(11) and 2.0484(11) in **49**, *cf.* Σr_{cov}(Pd,O) 2.05 Å⁶⁰) and with the *ortho* carbon from the arylidene ring (1.9654(17) in **52**, 1.9706(19) in **53**, 1.9746(13) in **49**, *cf.* Σr_{cov}(Pd,C) 2.12 Å⁶⁰). As a consequence, the geometry around the metal is distorted square planar. Between the three compounds the angles and the bond distances are very similar. The imidazolone or thiazolone groups are no longer planar but it adopts a U-shaped form. The corresponding imidazolone or thiazolone acts as a C^N-chelating ligand forming two six-membered PdNC4 chelate rings. The relative arrangement of the two orthopalladated ligands is transoid as confirmed by the single peaks in the ¹⁹F NMR spectra as well as the propyl resonances in the ¹H NMR spectrum of the imidazolone **49**.

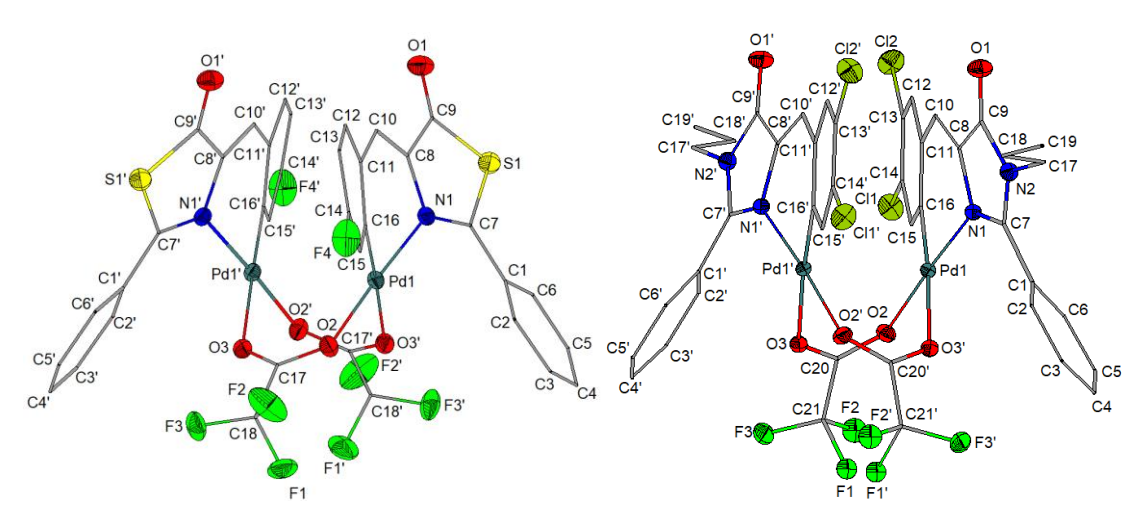


Figure 102. ORTEP-like representation (50% probability ellipsoids) of dimers in compounds 52 (left) and compound 49 (right). Hydrogen atoms were omitted for clarity.

The supramolecular architecture of the compounds **52** and **49** reveals the formation of chain-like associations through O···H contacts of 2.531(2) Å (H4···O3") (*cf.* $\Sigma r_{vdW}(O,H)$ 2.70 Å⁵⁹, $\Sigma r_{cov}(O,H)$ 0.97 Å⁶⁰) in **52** and 2.516(9) Å (H4···O3") in **49**. These contacts are formed between oxygen of the trifluoro acetato group and hydrogen atoms from the phenyl group. In compound **49** due to the additional propyl group in the imidazolone, H··· π interactions of 2.869(2) Å (H17B···Cg") give rise to a 2D network.

Finally in all three compounds the halogen attached to the arylidene ring is involved in F···H contacts of 2.568(3) Å (H5···F4") in **52** and F···Cl contacts of 3.066(2) Å (Cl1··· F2") (*cf.* $\Sigma r_{vdW}(F,Cl)$ 3.28 Å⁵⁹, $\Sigma r_{cov}(F,Cl)$ 1.59 Å⁶⁰) in **53** (**Figure 108**), that lead to a 3D supramolecular structure.

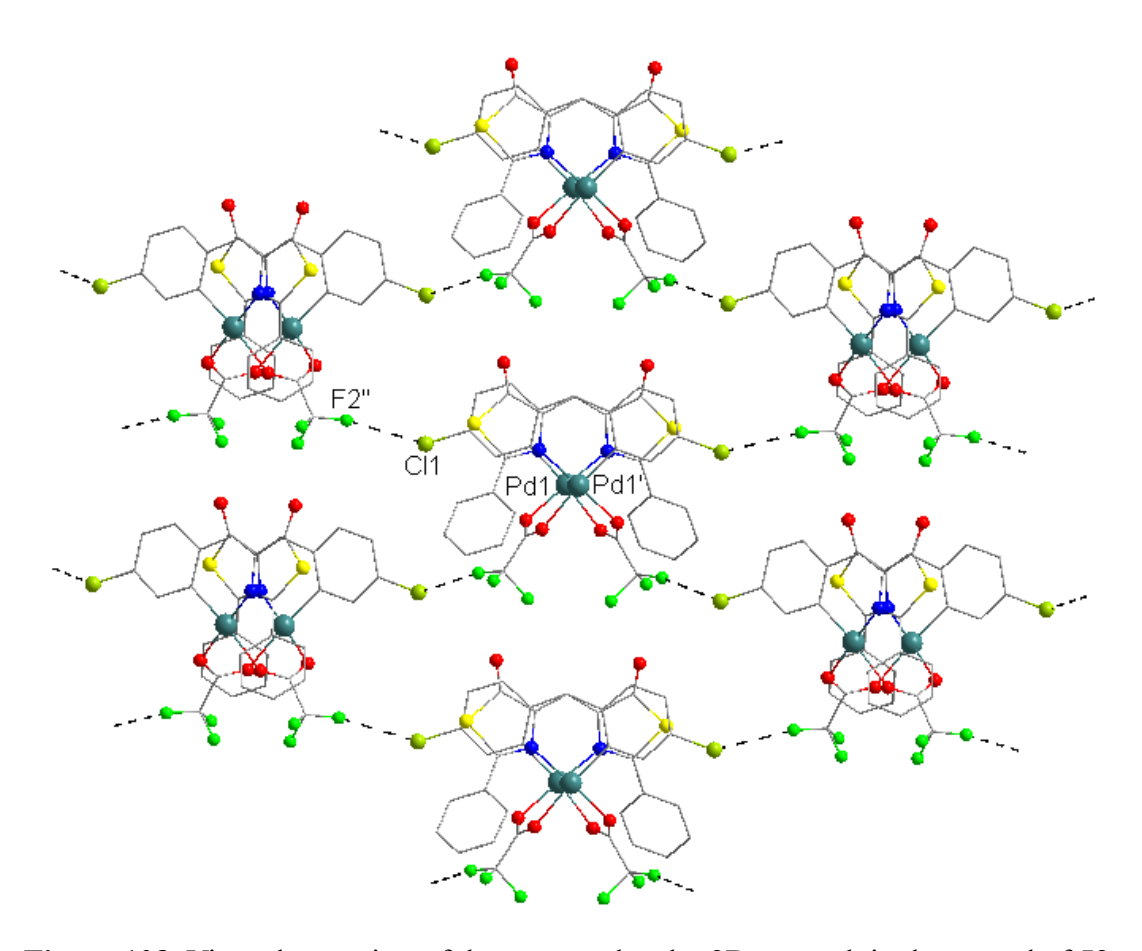


Figure 108. View along axis c of the supramolecular 2D network in the crystal of **53.** Hydrogen atoms that are not involved in intermolecular interactions were omitted for clarity. Symmetry equivalent atoms (1-x, y, 3/2-z) and (-1/2+x, 1/2+y, 3/2-z) are given are given by "prime" and "double prime", respectively.

Crystals suitable for X-ray diffraction studies upon compound 50a were isolated from the resulting mixture of reaction obtained from the synthesis of compound 50, during the attempts to change the ancillary ligand. The structure of compound 50a presented two independent molecules, 50a1 and 50a2 (Figure 109). The pyridine group is attached to the palladium center instead of a second trifluoroacetate group as it is in the orthopalladated dimers.

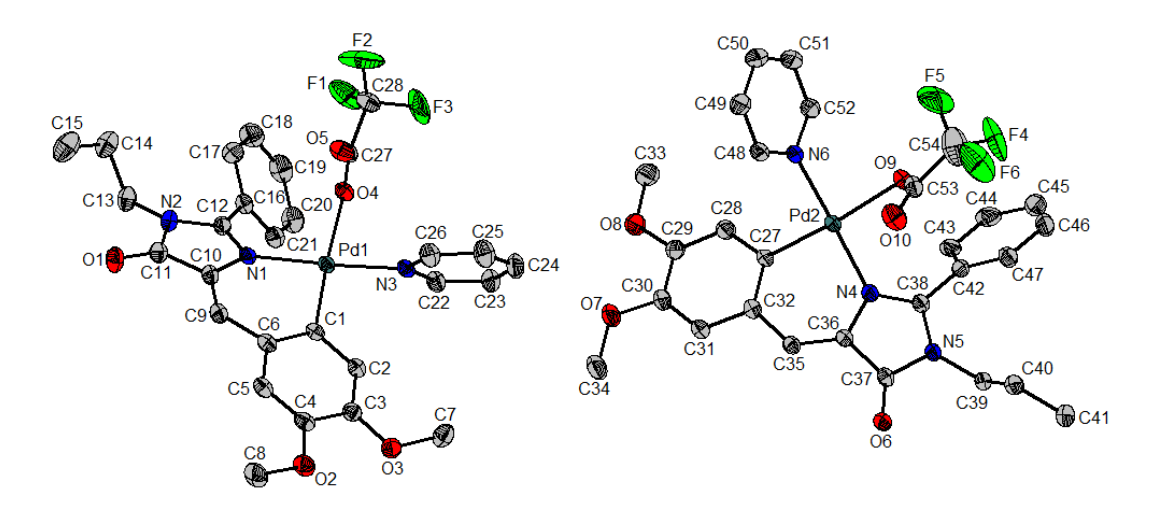


Figure 109. ORTEP-like representation (50% probability ellipsoids) of the independent molecules **50a1** (left) and **50a2** (right). Hydrogen atoms were omitted for clarity.

The square planar geometry around the palladium is closer to perfect configuration as compared with the orthopalladated dimers. Each independent molecule is involved in O···H interactions of 2.350(2) Å (H26···O1") in case of **50a1** and respectively 2.425(2) Å (H48"···O6') and 2.414(2) Å (H31"···O10') in case of **50a2** (*cf.* Σr_{vdW}(O,H) 2.70 Å⁵⁹, Σr_{cov}(O,H) 0.97 Å⁶⁰) with the same neighboring independent molecule (*i.e.* **50a1** with **50a1** and **50a2** with **50a2**) (**Figure 110**). The independent molecules are also involved in O···H interactions of 2.514(2) Å (H49'···O4) and 2.340(2) Å (H23···O10') between them (*i.e.* **50a1** with **50a2**) (**Figure 110**).

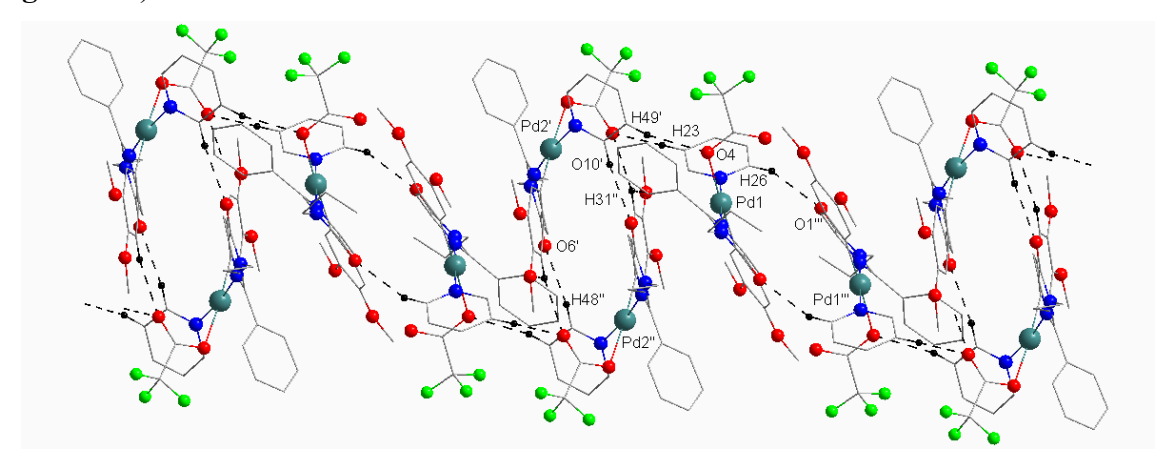


Figure 110. O···H interactions between the independent molecules of compound 50a. Symmetry equivalent atoms (-1+x, y, z), (1-x, 1-y, 1-z) and (-x, 1-y, 2-z) are given by "prime", "double prime" and "triple prime", respectively. Hydrogen atoms not involved in intermolecular interactions were omitted for clarity.

As a consequence, the independent molecules form a long chain structure in an alternating fashion through the O···H interactions shown previously. The chains are further

connected through other O···H interactions of 2.414(2) Å (H24···O8). The resulting 2D network is connected through F···H interactions of 2.419(12) Å (H45···F1"") (*cf.* $\Sigma r_{vdW}(F,H)$ 2.66 Å⁵⁹, $\Sigma r_{cov}(F,H)$ 0.88 Å⁶⁰) to form a 3D architecture.

The UV-Vis spectra of compounds 47, 48 and 49 presented a band at approximately 375 nm (374, 378 and 380 respectively) while compounds 50 and 51 presented a band at approximately 405 nm (400 and 407 respectively). The shift of the band is correlated with the electronic character of the substituents attached to the arylidene ring. In this case the compounds 50 and 51, having electronic donating groups (OMe), are more red shifted than compounds 47, 48 and 49, having electronic withdrawing groups (F, Cl). The strongest absorption maxima in the UV region of the spectrum, corresponds to a π - π * charge transfer from the 4-arylidene ring to the imidazolone heterocyclic moiety.

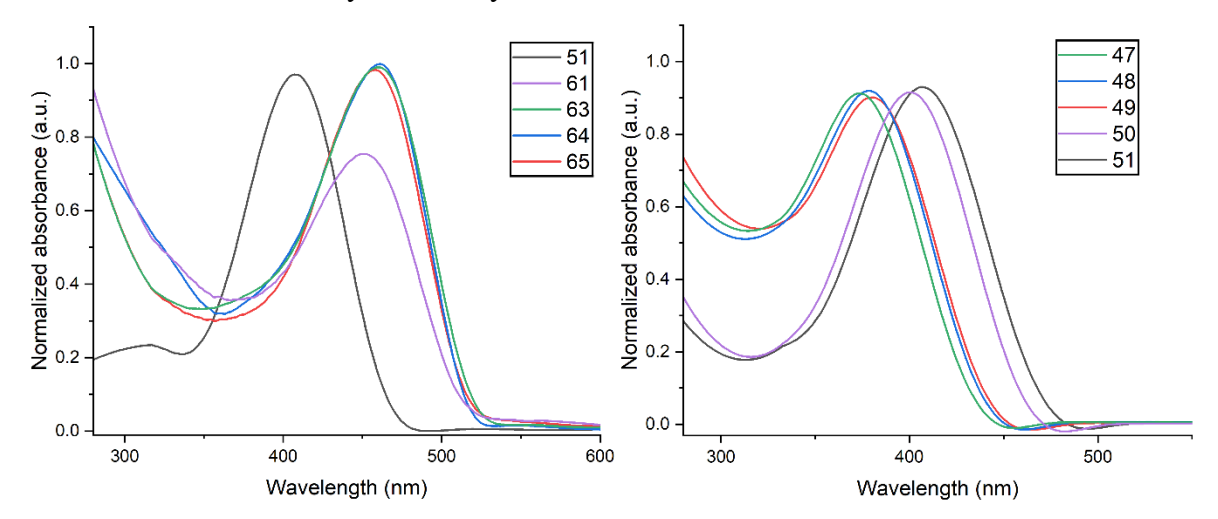


Figure 113. UV-Vis absorption spectra of compounds 47, 48, 49, 50 and 51 (left) and 51, 61, 63, 64 and 65 (right).

If we compare the orthopalladated compound **51** containing the trifluoroacetate bridge with compounds **61**, **63**, **64** and **65**, where the trifluoroacetate is changed with other ancillary ligands, the absorption band is even more red shifted from 407 nm to at approximately 455 nm (451, 459, 460 and 461 respectively) (**Figure 113**).

The excitation-emission spectra of **47**, **48**, **49**, **50** and **51** is characterized by a relatively large Stokes shift ranging between 3500 cm⁻¹ and 4700 cm⁻¹ while in compound **61**, **63**, **64** and **65** the Stokes shift is smaller ranging between 2500 cm⁻¹ and 2800 cm⁻¹. The excitation bands closely match the corresponding absorption bands.

The quantum yield (Φ_{PL}) values range from 2% to 15% for complexes **61**, **63**, **64** and **65**, where we have different ancillary ligands, while it is close to zero for the starting imidazolone **51** (<1%) as well as for the other imidazolones **47**, **48** and **49**, except for the

compound **50** with a Φ_{PL} of 5%. Therefore, we can say certainly that a true recovery of the fluorescence has been achieved and conclude that the change of ligands attached to the Pd atom has influenced the Φ_{PL} . Complex **64**, having the acetylacetonato ligand, exhibited the lowest Φ_{PL} (2%) out of the four complexes, followed by complex **61** with trifluoroacetate and pyridine (5%), complex **63** with trifluoroacetate and Cl (7%) and lastly complex **65** with the two pyridines having the best performance with a Φ_{PL} as high as 15%.

In order to provide more information about the role of the Pd and the ancillary ligands on the fluorescence, computational methods (DFT and TDDFT) were used for compounds 61, 63 and 65 which had the best Φ_{PL} . The absorption properties correspond to the excitation from the ground state (S₀) to the first excited singlet state (S₁), predominantly involving a HOMO to LUMO transition. In **Figure 116** there is detailed the HOMO orbitals with the percentage of the participation of the Pd orbitals (black) and the metallated carbon (red).

The results suggest a correlation between the participation of the Pd and C in the HOMO orbital and the value of the quantum yield measured experimentally. The values of Pd and C participations in compounds **61** (4.8% and 3.5%) and **63** (4.7% and 3.7%) are close to each other as there are the Φ_{PL} values (5% and respectively 7%). In contrast, in compound **65** the Pd and C participations are lower than the two and as observed the Φ_{PL} is considerably higher. This confirms that the lower the Pd and metallated carbon orbitals participation the higher the quantum yield.

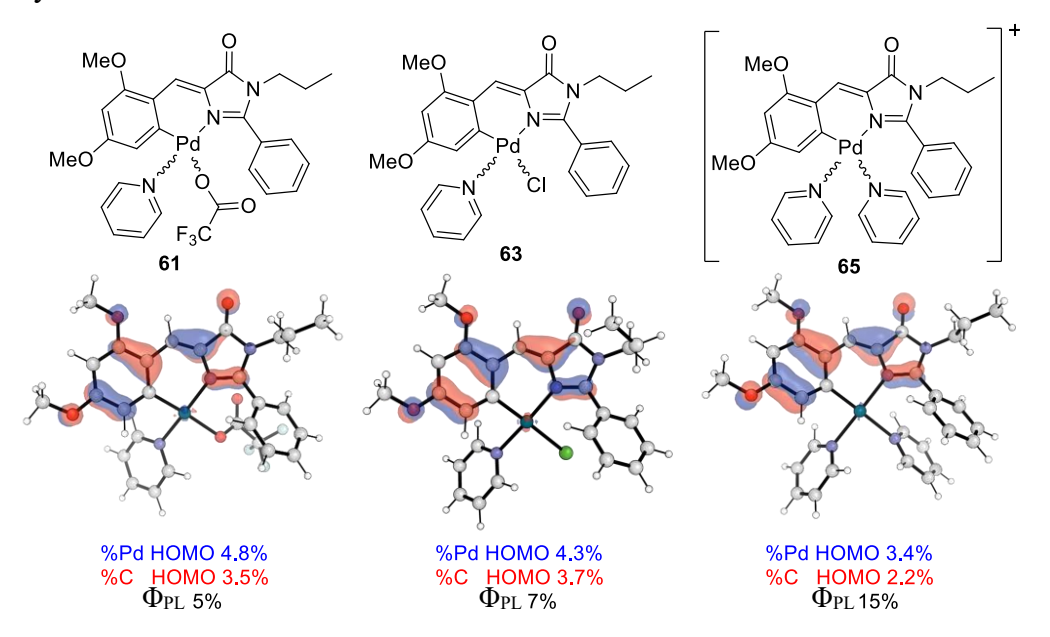


Figure 116. HOMO orbitals with the corresponding Pd contributions (blue) and orthopalladated C atom (red) of compounds **61**, **63** and **65**.

V. CONCLUSIONS

The present work has brought contributions to the field of chemistry researching the organic and organometallic compounds. The tasks achieved here were synthesizing the compounds, structurally characterizing them, evaluating their reactivity and, most important, testing their optical properties.

The main focus in subchapter III.1 was to obtain new diorganoselenides and to investigate their optical properties. Two types of diorganoselenium compounds were synthesized: R-Se-R (diorganoselenides containing benzaldehyde or 4-arylidene-5(4*H*)-oxazolone fragments) and R-Se-CH₂-Py-CH₂-Se-R (pyridine based compounds functionalized with two organoselenium side arms).

The diorganoselenides 1-4 containing benzaldehyde or dioxolane moieties were synthesized following or adapting the literature procedures. The oxazolones 5 and 6 were synthesized using the Erlenmeyer-Plöchl method. This compounds were further used to obtain complexes 7-16 by reaction with silver, gold and zinc salts. The diorganodiselenides 17, 18 and 19 were used as precursors for the synthesis of the new pyridine based compounds 20, 21 and 22 which were further used in complexation reactions with group 11 metal [silver(I) and copper(I)] to obtain complexes 23-31.

The ¹H and ¹³C NMR spectra revealed the formation of each class of compounds **1-16** and **17-31**, confirmed by the characteristic resonances and also supported by the the ⁷⁷Se NMR spectra. The ⁷⁷Se NMR of the complexes of ligands **5** and **6** showed no chemical shift of the selenium resonance signal as compared with the ligand which suggests that the metal interacts only with nitrogen and that a dynamic behavior in solution is occurring. In comparison, the complexes of ligand **20** and **22** the resonance signal of the selenium is considerably shifted which confirms the interaction of the metal with selenium in solution.

For the new compounds the characterization was completed by mass spectrometry where in all cases the pseudo-molecular ion was observed and molar conductibility consistent with either 1:1, 1:2 electrolytes or non-electrolyte behavour as expected.

In the solid state structure of the benzaldehyde 4 and the oxazolone 5 the selenium atom has a bent geometry. In case of compound 4 the oxygen is involved in O···H interactions, thus establishing supramolecular networks. In the solid state only one of nitrogen is coordinated to the metal in complex 9. The structure adopted a supramolecular association, in which two organoselenium ligands are coordinated to a tetranuclear silver core. The coordination geometry

around each silver center is a distorted square pyramid with no Ag···Ag interactions. A supramolecular 3D architecture determined by O···H, Cl···H and F···H secondary interactions was found in the crystal of complex 9.

The single-crystal X-ray diffraction studies for compounds **20** and **21** revealed supramolecular architectures formed by N···H intermolecular interactions, namely polymeric chains in the crystal of **20** and a 2D network in compound **21**.

In the crystals of complexes 24, 25 and 27 the molecules are associated, i.e. in dimeric units in compound 24, and in polymeric chains in compound, 25 and 27. Ag···Ag interactions were observed in compound 24. The resulting geometry around the metal center in compound 24 is a trigonal prism, in compounds 25 and 27 a square pyramid.

In the structure of compound **30** the resulting geometry around the copper center is a trigonal pyramid, where the selenium from one of the pendant arm and the nitrogen from the other pendant arm as well as the nitrogen from the pyridine are coordinated. The resulting 3D supramolecular architecture is achieved through weak I···Se and I···H contacts.

The UV-Vis absorption spectra the ortho-substituted species 5 presented a bigger bathochromic shift than the para-substituted species 6. The complexes showed similar emission maxima compared to the ligand, except compounds 8 and 14, which did not present fluorescence emission. A hyperchromic shift was observed for the complexes 12 and 16 when compared to the ligand. UV-Vis absorption spectra of the complexes 23-31 showed changes in the absorption maxima compared to the ligands 20-22.

In the subchapter III.2 are presented a series of 4-arylidene-5(4*H*)-imidazolones and 4-arylidene-5(4*H*)-thiazolones. First the thiazolones and imidazolones ligands and palladium complexes were synthesized and characterized and then their photochemical and photophysical properties were tested.

The starting oxazolones 32-36 were synthesized according to a previously reported method. The oxazolones were further used as starting materials for the synthesis of a series of imidazolones (compounds 37-41) and thiazolones (compounds 42-46), which were obtained according or adapted to the previously reported methods. The orthopalladated imidazolones and thiazolones 47-55 were synthesized. The photochemical reactivity of these compounds was tested. Only compounds 47, 48, 49, 53, 54 underwent [2+2]-cycloaddition, thus enabling the synthesis of compounds 56-60. For compound 51 a change of the ancillary ligands was employed and compounds 61-65 were synthesized, therefore. All compounds were fully characterized using NMR spectroscopy and mass spectrometry (except for compound 62 where NMR spectroscopy was not possible and instead infrared spectroscopy was employed).

The NMR spectra of compounds 47-55 showed the formation of dimers as a result of the C-H activation with palladium of the ligands resulting in an *anti* arrangement of the orthopalladated moieties. They are in accordance with the differences determined by the different substituents and the presence of either thiazolones or imidazolones in the molecule. The NMR studies of the [2+2]-cycloaddition products confirmed the formation of the cyclobutane by the drastic chemical shift change of the methine protons. In case of compounds 61, 63, and 65 the NMR studies revealed a dynamic behavior in solution at room temperature with the formation of *cis* and *trans* isomers.

The X-ray crystal structure of compounds 49, 52 and 53 confirmed the *anti* arrangement and two independent monomeric molecules of compound 50a.

Imidazolones 47-51 and 61-65 were characterized by UV-Vis spectroscopy. The photophysical characterization revealed emission maxima in the visible light region. The shift of the bands was correlated with the electronic character of the substituents attached to the arylidene ring. The compounds with electronic donating groups were more red shifted than the compounds with electronic withdrawing groups. The change of the ancillary ligands in palladium complexes showed good results with a quantum yield turnover up to 15% compared with <1% of the initial imidazolone. Making use of the computational calculations for compounds 61, 63 and 65 we could conclude that the lower the Pd and metallated carbon orbitals participation the higher the electron density of the imidazolone ligand and thus the higher the quantum yield.

VI.REFERENCES

- 1. M. de Bruin, Pure Appl. Chem., 1982, 54, 1533.
- 2. K.-D. Gundermann, *Chemilumineszenz organischer Verbindungen*, p. 2, Springer, Berlin, **1968**.
- 3. B. Valeur, M. N. Berberan-Santos, J. Chem. Educ., 2011, 88, 731.
- 4. P. S. Francis, C. F. Hogan, Compr. Anal. Chem., 2008, 13, 343.
- L. N. Viana, A. P. S. Soares, D. L. Guimarães, W. J. S. Rojano, T. D. Saint' Pierre, J. Environ. Chem. Eng., 2022, 10, 108915.
- 6. N. Senesi, V. D'Orazio, *Encyclopedia of Soils in the Environment*, p. 35, Elsevier, Oxford, **2005**.
- 7. A. Bose, I. Thomas, G. Kavitha, E. Abraham, Int. J. Adv. Pharm. Res., 2018, 8, 1.
- 8. A. Shahzad, G. Köhler, M. Knapp, E. Gaubitzer, M. Puchinger, M. Edetsberger, *J. Transl. Med.*, **2009**, 7, 99.
- 9. L. Marcu, Ann. Biomed. Eng., 2012, 40, 304.
- 10. H. Sahoo, *RSC Adv.*, **2012**, 2, 7017.
- 11. J. H. Correia, J. A. Rodrigues, S. Pimenta, T. Dong, Z. Yang, *Pharmaceutics.*, **2021**, 13, 1332.
- 12. L. Reiß, T. Prestel, S. Giering, *Herit. Sci.*, **2022**, 10, 171.
- 13. W. Li, J. Wang, Y. Xie, M. Tebyetekerwa, Z. Qiu, J. Tang, S. Yang, M. Zhu, Z. Xu, *Progress in Organic Coatings*, **2018**, 120, 1.
- 14. Y.-L. Wang, C. Li, H.-Q. Qu, C. Fan, P.-J. Zhao, R. Tian, M.-Q. Zhu, *J. Am. Chem. Soc.*, **2020**, 142, 7497.
- 15. C. Sun, W. Shi, Y. Song, W. Chen, H. Ma, Chem. Commun., 2011, 47, 8638.
- 16. W. Shi, S. Sun, X. Li, H. Ma, *Inorg. Chem.*, **2010**, 49, 1206.
- 17. Z. Lou, P. Li, Q. Panab, K. Han, Chem. Commun., 2013, 49, 2445.
- 18. G. Cheng, J. Fan, W. Sun, J. Cao, C. Hu, X. Peng, *Chem. Commun.*, **2014**, 50, 1018.
- 19. G. Li, D. Zhu, Q. Liu, L. Xue, H. Jiang, Org. Lett., 2013, 15, 2002.
- 20. X.-H. Xu, C. Liu, Y. Meia, Q.-H. Song, J. Mater. Chem. B, 2019, 7, 6861.
- 21. S.-R. Liu, S.-P. Wu, Org. Lett., 2013, 15, 878.
- 22. S. V. Mulay, T. Yudhistira, M. Choi, Y. Kim, J. Kim, Y. J. Jang, S. Jon, D. G. Churchill, *Chem. Asian J.*, **2016**, 11, 3598.
- 23. D. S. Shelar, G. S. Malankar, M. Manikandan, M. Patra, R. J. Butcher, S. T. Manjare, *New J. Chem.*, **2022**, 46, 17610.

- 24. G. S. Malankar, A. Sakunthala, A. Navalkar, S. K. Maji, S. Raju, S. T. Manjare, *Anal. Chim. Acta*, **2021**, 1150, 338205.
- 25. W. Zhang, W. Liu, P. Li, J. Kang, J. Wang, H. Wang, B. Tang, *Chem. Commun.*, **2015**, 51, 10150.
- 26. S. Zang, X. Kong, J. Cui, S. Su, W. Shu, J. Jing, Xi. Zhang, *J. Mater. Chem. B*, **2020**, 8, 2660.
- X. Chen, K.-A. Lee, E.-M. Ha, K. M. Lee, Y. Y. Seo, H. K. Choi, H. N. Kim, M. J. Kim,
 C.-S. Cho, S. Y. Lee, W.-J. Lee, J. Yoon, *Chem. Commun.*, 2011, 47, 4373.
- 28. B. Wang, P. Li, F. Yu, J. Chen, Z. Qu, K. Han, Chem. Commun., 2013, 49, 5790.
- 29. S. Huang, S. He, Y. Lu, F. Wei, X. Zeng, L. Zhao, Chem. Commun., 2011, 47, 2408.
- 30. S. Panda, P.B. Pati, S.S. Zade, Chem. Commun., 2011, 47, 4174.
- 31. A. Kumar, J.D. Singh, *Inorg. Chem.*, **2012**, 51, 772.
- 32. Y. Li, S. He, Y. Lu, X. Zeng, Org. Biomol. Chem., 2011, 9, 2606.
- 33. K. Mariappan, P. N. Basa, V. Balasubramanian, S. Fuoss, A. G. Sykes, *Polyhedron*, **2013**, 55, 144.
- 34. D. P. Murale, S. T. Manjare, Y.-S. Lee, D. G. Churchill, *Chem. Commun.*, **2014**, 50, 359.
- 35. C.-Y. Chou, S.-R. Liu, S.-P. Wu, *Analyst*, **2013**, 138, 3264.
- 36. J. Tian, H. Chen, L. Zhuo, Y. Xie, N. Li, B. Tang, *Chem. Eur. J.*, **2011**, 17, 6626.
- 37. B. Wang, F. Yu, P. Li, X. Sun, K. Han, *Dyes Pigments*, **2013**, 96, 383.
- 38. F. Yu, P. Li, G. Li, G. Zhao, T. Chu, K. Han, J. Am. Chem. Soc., 2011, 133, 11030.
- 39. C. Sun, W. Du, P. Wang, Y. Wu, B. Wang, J. Wang, W. Xie, *Biochem. Biophys. Res. Commun.*, **2017**, 494, 518.
- 40. M. B. Halle, K. Jin Lee, T. Yudhistira, J. H. Choi, H.-S. Park, D. G. Churchill, *Chem. Asian J.*, **2018**, 13, 3895.
- 41. I. C. Mondal, M. Galkin, S. Sharma, N. A. Murugan, D. A. Yushchenko, K. Girdhar, A. Karmakar, P. Mondal, P. Gaur, S. Ghosh, *Chem Asian J.*, **2022**, 17, e202101281.
- 42. D. Gong, X. Zhu, Y. Tian, S.-C. Han, M. Deng, A. Iqbal, W. Liu, W. Qin, H. Guo, *Anal. Chem.*, **2017**, 89, 1801.
- 43. A. J. Mukherjee, S. S. Zade, H. B. Singh, R. B. Sunoj, *Chem. Rev.*, **2010**, 110, 4357.
- 44. S. Panda, A. Panda, S. S. Zade, Coord. Chem. Rev., 2015, 300, 86.
- 45. A. Panda, S. C. Menon, H. B. Singh, R. J. Butcher, *J. Organomet. Chem.*, **2001**, 623, 87.
- 46. A. Panda, G. Mugesh, H. B. Singh, R. J. Butcher, Organometallics, 1999, 18, 1986.
- 47. H.Shirani, T. Janosik, Organometallics, 2008, 27, 3960.

- 48. B. K. Sarma, D. Manna, M. Minoura, G. Mugesh, J. Am. Chem. Soc., 2010, 132, 5364.
- 49. S. K. Tripathi, U. Patel, D. Roy, R. B. Sunoj, H. B. Singh, G. Wolmershäuser, R. J. Butcher, *J. Org. Chem.*, **2005**, 70, 9237.
- 50. S. S. Zade, S. Panda, H. B. Singh, G. Wolmershäuse, Tetrahedron Lett., 2005, 46, 665.
- 51. T. Chakraborty, S. Sharma, H. B. Singh, R. J. Butcher, *Organometallics*, **2011**, 30, 2525.
- 52. S. Zhang, K. Karra, C. Heintz, E. Kleckler, J. Jin, Tetrahedron Lett., 2013, 54, 4753.
- 53. N. Taniguchi, Synlett, 2005, 11, 1687.
- 54. D. Yadav, A. K. Dixit, S. Raghothama, S. K. Awasthi, *Dalton Trans.*, 2020, 49, 12266.
- 55. N. Taniguchi, *Tetrahedron*, **2016**, 72, 5818.
- 56. V. P. Reddy, A. V. Kumar, K. R. Rao, *J. Org. Chem.*, **2010**, 75, 8720.
- 57. W. Nakanishi, S. Hayashi, Y. Kusuyama, J. Chem. Soc., Perkin Trans. 2, 2002, 262.
- 58. S. Bhandary, A. Sirohiwal, R. Kadu, S. Kumar, D. Chopra, *Cryst. Growth Des.*, **2018**, 18, 3734.
- 59. S. Alvarez, *Dalton Trans.*, **2013**, 42, 8617.
- 60. B. Cordero, V. Gómez, A. E. Platero-Prats, M. Revés, J. Echeverría, E. Cremades, F. Barragán, S. Alvarez, *Dalton Trans.*, **2008**, 2832.
- 61. M.-H. Wu, W.-J. Liu, Acta Cryst., 2011, E67, o2983.
- 62. H. Bouraoui, A. Boudjada, S. Bouacida, Y. Mechehoudc, J. Meinnel, *Acta Cryst.*, **2011**, E67, o941.
- 63. R. A. Butuza, D. Dumitras, C. Bohan, A. Pop, New J. Chem., 2023, 47, 2202.
- 64. D. Dumitraș, A. Pop, A. Silvestru, *Polyhedron*, **2022**, 220, 115801.
- 65. Q. Yao, E. P. Kinney, C. Zheng, *Org. Lett.*, **2004**, 6, 2997.
- 66. D. Das, G. K. Rao, A. K. Singh, Organometallics, 2009, 28, 6054.
- 67. J. Aydin, N. Selander, K. J. Szabó, Tetrahedron Lett., 2006, 47, 8999.
- 68. A. Ilie, A. Laguna, C. Silvestru, C. R. Chim., 2012, 15, 895.
- 69. D. Das, P. Singh, O. Prakash, A. K. Singh, *Inorg. Chem. Commun.*, 2010, 13, 1370.
- 70. R. Kaur, H. B. Singh, R. P. Patel, J. Chem. Soc., Dalton Trans., 1996, 2719.
- 71. A. S. Hodage, C. P. Prabhu, P. P. Phadnis, A. Wadawale, K. I. Priyadarsini, V. K. Jain, *J. Organomet. Chem.*, **2012**, 720, 19.
- 72. M. Hojjatie, S. Muralidharan, H. Freiser, *Tetrahedron*, **1989**, 45, 1611.
- 73. A. Lari, R. Gleiter, F. Rominger, Eur. J. Org. Chem., 2009, 2267.
- 74. G. Roy, G. Mugesh, J. Am. Chem. Soc., 2005, 127, 15207.
- 75. M. Chalfie, Angew. Chem. Int. Ed., 2009, 48, 5603.
- 76. R.Y. Tsien, Angew. Chem. Int. Ed., 2009, 48, 5612.

- 77. M. Zimmer, Chem. Rev. 2002, 102, 759.
- 78. I. V. Yampolsky, A. A. Kislukhin, T. T. Amatov, D. Shcherbo, V. K. Potapov, S. Lukyanov, K. A. Lukyanov, *Bioorg. Chem.*, **2008**, 36, 96.
- 79. C. A. B. Rodrigues, I. F. A. Mariz, E. M. S. Maçôas, C. A. M. Afonso, J. M. G. Martinho, *Dyes Pigm.*, **2012**, 95, 713.
- 80. C. A. B. Rodrigues, I. F. A. Mariz, E. M. S. Maçôas, C. A. M. Afonso, J. M. G. Martinho, *Dyes Pigm.*, **2013**, 99, 642.
- 81. M. Blanco-Lomas, P. J. Campos, D. Sampedro, Org. Lett., 2012, 14, 4334.
- 82. M. Blanco-Lomas, I. Funes-Ardoiz, P. J. Campos, D. Sampedro, *Eur. J. Org. Chem.*, **2013**, 2013, 6611.
- 83. P. Krawczyk, M. Bratkowska, T. Wybranowski, I. Hołyńska-Iwan, P. Cysewski, B. Jędrzejewska, *J. Mol. Liq.*, **2020**, 314, 113632.
- 84. S. Sierra, D. Dalmau, S. Higuera, D. Cortés, O. Crespo, A. I. Jimenez, A. Pop, C. Silvestru, E. P. Urriolabeitia, *J. Org. Chem.*, **2021**, 86, 12119.
- 85. J. S. Paige, K. Wu, S. R. Jaffrey, Science, 2011, 333, 642.
- 86. H. Suna, H.-X. Lenga, J.-S. Liua, G. Roya, J.-W. Yana, L. Zhang, *Sens. Actuators, B*, **2020**, 305, 127509.
- 87. Y. Guo, H. Leng, Y. Wang, W.-J. Shi, L. Zhang, J. Yan, *Dyes Pigm.*, **2022**, 206, 110665.
- 88. H. Leng, J. Yang, L. Long, Y. Yan, W.-J. Shi, *Bioorg. Chem.*, **2023**, 136, 106540.
- 89. M. S. Baranov, K. M. Solntsev, N. S. Baleeva, A. S. Mishin, S. A. Lukyanov, K. A. Lukyanov, I. V. Yampolsky, *Chem. Eur. J.*, **2014**, 20, 13234.
- 90. Y. Zhou, Dai, J. Qi, J. Wu, Y. Huang, B. Shen, X. Zhi, Y. Fu, Spectrochim. Acta A Mol. Biomol. Spectrosc., 2023, 286, 121946.
- 91. H. Leng, Y. Wang, J. Wang, H. Sun, A. Sun, M. Pistolozzi, L. Zhang, J. Yan, *Anal. Chem.*, **2022**, 94, 1999.
- 92. L. L. Mittapellia, G. N. Nawaleb, S. P. Gholapc, O. P. Vargheseb, K. R. Gorea, *Sens. Actuators, B*, **2019**, 298, 126875.
- 93. I. N. Myasnyanko, A. S. Gavrikov, S. O. Zaitseva, A. Yu. Smirnov, E. R. Zaitseva, A. I. Sokolov, K. K. Malyshevskaya, N. S. Baleeva, A. S. Mishin, M. S. Baranov, *Chem. Eur. J.*, **2021**, 27, 3986.
- 94. A Y. Smirnov, M. M. Perfilov, E. R. Zaitseva, M. B. Zagudaylova, S. O. Zaitseva, A. S. Mishin, M. S. Baranov, *Dyes Pigm.*, **2020**, 177, 108258.
- 95. X. Li, H. Kim, J. L. Litke, J. Wu, S. R. Jaffrey, Angew. Chem. Int. Ed., 2020, 59, 4511.

- 96. M. M. Perfilov, E. R. Zaitseva, N. S. Baleeva, V. S. Kublitski, A. Y. Smirnov, Y. A. Bogdanova, S. A. Krasnova, I. N. Myasnyanko, A. S. Mishin, M. S. Baranov, *Int. J. Mol. Sci.*, **2023**, 24, 9923.
- 97. B. Shen, Y. Qian, Dyes Pigm., 2019, 166, 350.
- 98. N. V. Povarova, S. O. Zaitseva, N. S. Baleeva, A. Yu. Smirnov, I. N. Myasnyanko, M. B. Zagudaylova, N. G. Bozhanova, D. A. Gorbachev, K. K. Malyshevskaya, A. S. Gavrikov, A. S. Mishin, M. S. Baranov, *Chem. Eur. J.*, **2019**, 25, 9592.
- 99. A. Singh, G. Ramanathan, J. Lumin., 2017, 182, 220.
- 100. A. L. Mirajkar, L. L. Mittapelli, G. N. Nawale, K. R. Gore, *Sens. Actuators, B*, **2018**, 265, 257.
- C.-Y. Lin, M. G. Romei, L. M. Oltrogge, I. I. Mathews, S. G. Boxer, *J. Am. Chem. Soc.*,
 2019, 141, 15250.
- 102. A. Follenius-Wund, M. Bourotte, M. Schmitt, F. Iyice, H. Lami, J.-J. Bourguignon, J. Haiech, C. Pigault, *Biophys. J.*, **2003**, 85, 1839.
- 103. Y.-J. Ai, R.-Z. Liao, W.-H. Fang, Y. Luo, Phys. Chem. Chem. Phys., 2012, 14, 13409.
- 104. J. Chang, M. G. Romei, S. G. Boxer, J. Am. Chem. Soc., 2019, 141, 15504.
- 105. H. Deng, C. Yu, L. Gong, X. Zhu, J. Phys. Chem. Lett., 2016, 7, 2935.
- M. S. Baranov, K. A. Lukyanov, A. O. Borissova, J. Shamir, D. Kosenkov, L. V. Slipchenko, L. M. Tolbert, I. V. Yampolsky, K. M. Solntsev, *J. Am. Chem. Soc.*, 2012, 134, 6025.
- Y.-H. Hsu, Y.-A. Chen, H.-W. Tseng, Z. Zhang, J.-Y. Shen, W.-T. Chuang, T.-C. Lin, C.-S. Lee, W.-Y. Hung, B.-C. Hong, S.-H. Liu, P.-T. Chou, *J. Am. Chem. Soc.*, 2014, 136, 11805.
- N. S. Baleeva, S. O. Zaitseva, K. S. Mineev, A. V. Khavroshechkina, M. B. Zagudaylova,
 M. S. Baranov, *Tetrahedron Lett.*, 2019, 60, 456.
- 109. C. Chen, W. Liu, M. S. Baranov, N. S. Baleeva, I. V. Yampolsky, L. Zhu, Y. Wang, A. Shamir, K. M. Solntsev, C. Fang, *J. Phys. Chem. Lett.*, **2017**, 8, 5921.
- S. Collado, A. Pueyo, C. Baudequin, L. Bischoff, A. I. Jiménez, C. Cativiela, C. Hoarau,
 E. P. Urriolabeitia, *Eur. J. Org. Chem.*, 2018, 6158.
- 111. J. M. Lerestif, J. Perrocheau, F. Tonnard, J. P. Bazureau, J. Hamelin, *Tetrahedron*, **1995**, 51, 6757.
- 112. A. H. Harhash, N. A. L. Kassab, A. A. A. Elbanani, *Indian J. Chem.*, **1971**, 9, 789.
- 113. A. Kumar, M. Varma, A.K. Saxena, K. Shanker, *Indian J. Chem.*, **1988**, 27B, 301.
- 114. U. Wenge, H.-A. Wagenknecht, Synthesis, 2011, 3, 502.

- 115. P. K. Tripathy, A. K. Mukerjee, Synthesis, 1985, 285.
- 116. C.-Y. Lee, Y.-C. Chen, H.-C. Lin, Y. Jhong, C.-W. Chang, C.-H. Tsai, C.-L. Kao, T.-C. Chien, *Tetrahedron*, **2012**, 68, 5898.
- 117. M. Muselli, L. Colombeau, J. Hédouin, C. Hoarau, L. Bischoff, Synlett, 2016, 27, 2819.
- 118. A.H. Cook, G. Harris, I. Heilbron, G. Shaw, J. Chem. Soc., 1948, 1056.
- 119. R. Filler, Y. S. Rao, J. Org. Chem., 1962, 27, 3730.
- 120. G. Bhattacharjyaa, G. Savithaa, G. Ramanathan, J. Mol. Struct., 2005, 752, 98.
- 121. G.-D. Roiban, E. Serrano, T. Soler, G. Aullón, I. Grosu, C. Cativiela, M. Martínez, E. P. Urriolabeitia, *Inorg. Chem.*, **2011**, 50, 8132.
- 122. D. Dalmau, O. Crespo, J. M. Matxain, E. P. Urriolabeitia, Inorg. Chem., 2023, 62, 9792.
- 123. C. Garcia-Sanz, A. Andreu, B. de las Rivas, A. I. Jimenez, A. Pop, C. Silvestru, E. P. Urriolabeitia, J. M. Palomo, *Org. Biomol. Chem.*, **2021**, 19, 2773.
- 124. A. Panda, S. C. Menon, H. B. Singh, R. J. Butcher, *J. Organomet. Chem.*, **2001**, 623, 87.
- 125. a) J. Plöchl, Ber. Dtsch. Chem. Ges., 1883, 16, 2815; (b) J. Plöchl, Ber. Dtsch. Chem. Ges., 1884, 17, 1623; (c) E. Erlenmeyer, Justus Liebigs Ann. Chem., 1893, 275, 1; (d) J. S. Buck, W. S. Ide, Org. Synth., 1933, 13, 8.
- 126. S. Bhandary, A. Sirohiwal, R. Kadu, S. Kumar, D. Chopra, *Cryst. Growth Des.*, **2018**, 18, 3734.
- D.-H. Wang, Y. Zhang, Y.-T. Wang, H.-Y. Feng, Y. Chen, D.-Z. Zhao, *ChemPlusChem*,
 2017, 82, 323.
- 128. S. Kumar, H. B. Singh, G. Wolmershauser, Organometallics, 2006, 25, 382.
- 129. S. D. Apte, S. S. Zade, H. B. Singh, R. J. Butcher, *Organometallics*, **2003**, 22, 5473.
- 130. S. J. Angus-Dunne, L. E. P. Lee Chin, R. C. Burns, G. A. Lawrance, Transit. *Met. Chem.*, **2006**, 31, 268.
- 131. X. Xuana, J. Wang, H. Wang, Electrochim. Acta, 2005, 50, 4196.
- 132. L. D. Kock, M. D. S. Lekgoathi, P. L. Crouse, B. M. Vilakazi, *J. Mol. Struct.*, **2012**, 1026, 145.
- 133. I. Ali, W. A. Wani, K. Saleem, *Synth. React. Inorg., Met.-Org., Nano-Met. Chem.*, **2013**, 43, 1162.
- 134. K. A. Hirsch, S. R. Wilson, J. S. Moore, *Inorg. Chem.*, **1997**, 36, 2960.
- 135. A. W. Addison, T. N. Rao, J. Reedijk, J. van Rijn, G. C. Verschoor, *J. Chem. Soc.*, *Dalton Trans.*, **1984**, 1349.

- 136. R. A. Popa, E. Licarete, M. Banciu, A. Silvestru, *Appl. Organomet. Chem.*, **2018**, 32, E4252.
- 137. A. S. Hodage, C. P. Prabhu, P. P. Phadnis, A. Wadawale, K. I. Priyadarsini, V. K. Jain, J. Organomet. Chem., 2012, 720, 19.
- 138. R. Kaur, H. B. Singh, R. P. Patel, J. Chem. Soc., Dalton Trans., 1996, 2719.
- 139. I. C. Berdiell, S. L. Warriner, M. A. Halcrow, Dalton Trans., 2018, 47, 5269.
- 140. E. I. Stiefel, G.F. Brown, Inorg. Chem., 1972, 11, 434.
- 141. F. Pointillart, P. Herson, K. Boubekeur, C. Train, *Inorg. Chim. Acta*, 2008, 361, 373.
- 142. W.-W. du Mont, A. Martens-von Salzen, F. Ruthe, E, Seppälä, G, Mugesh, F. A. Devillanova, V. Lippolis, N. Kuhn, *J. Organomet. Chem.*, **2001**, 623, 14.
- 143. M. Muselli, L. Colombeau, J. Hédouin, C. Hoarau, L. Bischoff, Synlett, 2016, 27, 2819.
- 144. S. Sierra, D. Dalmau, S. Higuera, D. Cortés, O. Crespo, A. I. Jimenez, A. Pop, C. Silvestru, E. P. Urriolabeitia, J. Org. Chem., 2021, 86, 12119.
- 145. K. Manabu, H. Ryoichi, T. Mitsuo, W., Tatsuo, S. Hiroyuki, J. of Phys, Chem., 1995, 14784.
- 146. C. Cativiela, M. D. Díaz de Villegas, E. Meléndez, *J. Heterocycl. Chem.*, **1985**, 22, 1655.
- 147. S. Feng, Z. Junyong, T. Shujiang, J. Runhong, Z. Yan, J. Bo, J. Hong, *J. Heterocycl. Chem.*, **2007**, 44, 1013.
- 148. Y. S. Rao, R. Filler, Synthesis, 1975, 12, 749.
- 149. V. A. Deulofeu, An. R. Soc. Esp. Fis. Quim., 1934, 32, 152.
- 150. P. N. Rodríguez, O. Ghashghaei, A. M. Schoepf, S. Benson, M. Vendrell, R. Lavilla, *Angew. Chem. Int. Ed.*, **2023**, 62, e202303889.
- 151. S. Sierra, M. V. Gomez, A. I. Jiménez, A. Pop, C. Silvestru, M. L. Marín, F. Boscá, G. Sastre, E. Gómez-Bengoa, E. P. Urriolabeitia, *J. Org. Chem.*, **2022**, 87, 3529.
- 152. A. García-Montero, A. M. Rodriguez, A. Juan, A. H. Velders, A. Denisi, G. Jiménez-Osés, E. Gómez-Bengoa, C. Cativiela, M. V. Gómez, E. P. Urriolabeitia, ACS Sustainable Chem. Eng., 2017, 5, 8370.
- 153. D. Roiban, E. Serrano, T. Soler, I. Grosu, C. Cativielad, E. P. Urriolabeitia, *Chem. Commun.*, **2009**, 4681.
- 154. C. Carrera, A. Denisi, C. Cativiela, E. P. Urriolabeitia, Eur. J. Inorg. Chem., 2019, 3481.
- 155. E. P. Urriolabeitia, P. Sánchez, A. Pop, C. Silvestru, E. Laga, A. I. Jiménez, C. Cativiela, *Beilstein J. Org. Chem.*, **2020**, 16, 1111.

- E. Serrano, A. Juan, A. García-Montero, T. Soler, F. Jiménez-Márquez, C. Cativiela, M. V. Gomez, E. P. Urriolabeitia, *Chem. Eur. J.*, 2016, 22, 144.
- 157. C. Garcia-Sanz, A. Andreu, B. de las Rivas, A. I. Jimenez, A. Pop, C. Silvestru, E. P. Urriolabeitia, J. M. Palomo, *Org. Biomol. Chem.*, **2021**, 19, 2773.
- 158. D. Dalmau, O. Crespo, J. M. Matxain, E. P. Urriolabeitia, *Inorg. Chem.*, 2023, 62, 9792.
- 159. E. Laga, D. Dalmau, S. Arregui, O. Crespo, A. I. Jimenez, A. Pop, C. Silvestru, E. P. Urriolabeitia, *Molecules*, **2021**, 26, 1238.
- S. Collado, A. Pueyo, C. Baudequin, L. Bischoff, A. I. Jiménez, C. Cativiela, C. Hoarau,
 E. P. Urriolabeitia, Eur. J. Org. Chem., 2018, 6158.
- 161. K. E. Horner, P. B. Karadakov, J. Org. Chem., 2015, 80, 7150.
- 162. H. Hiemstra, H. A. Houwing, O. Possel, A. M. van Leusen, *Can. J. Chem.*, **1979**, 57, 3168.
- 163. E. Pretsch, P. Bühlmann, M. Badertscher, *Structure Determinationof Organic Compounds*, p. 269, Springer, Berlin, **2009**.
- 164. O. Foss, J. J. Pitha, *Inorg. Synt.*, **1953**, 4, 91.
- 165. L. Kiss, A. Pop, S. Sergiu, C. I. Rat, C. Silvestru, *Appl. Organomet. Chem.*, **2021**, 35, e6339.
- 166. R. Uson, A. Laguna, M. Laguna, Inorg. Synth., 1989, 26, 85
- 167. MestReC; MestReNova; Mestrelab Research S.L. *A Coruna 15706*, version 14; Mestrelab Research: Santiago de Compostela, Spain, **2020**.
- 168. A. L. Spek, J. Appl. Cryst., 2003, 36, 7.
- 169. A. L. Spek, Acta Cryst., 2009, D65, 148.
- 170. W. T. Pennington, DIAMOND Visual Crystal Structure Information System; Crystal Impact: Bonn, Germany, **2001**.
- 171. (a) P. Hohenberg, W. Kohn, *Phys. Rev.*, **1964**, 136, B864; (b) W. Kohn, L. J. Sham, *Phys. Rev.*, **1965**, 140, A1133.
- 172. Gaussian 16, Revision C.01, M. J. Frisch, G. W. Trucks, H. B. Schlegel, G. E. Scuseria, M. A. Robb, J. R. Cheeseman, G. Scalmani, V. Barone, G. A. Petersson, H. Nakatsuji, X. Li, M. Caricato, A. V. Marenich, J. Bloino, B. G. Janesko, R. Gomperts, B. Mennucci, H. P. Hratchian, J. V. Ortiz, A. F. Izmaylov, J. L. Sonnenberg, D. Williams-Young, F. Ding, F. Lipparini, F. Egidi, J. Goings, B. Peng, A. Petrone, T. Henderson, D. Ranasinghe, V. G. Zakrzewski, J. Gao, N. Rega, G. Zheng, W. Liang, M. Hada, M. Ehara, K. Toyota, R. Fukuda, J. Hasegawa, M. Ishida, T. Nakajima, Y. Honda, O. Kitao, H. Nakai, T. Vreven, K. Throssell, J. A. Montgomery Jr., J. E. Peralta, F. Ogliaro, M. J.

- Bearpark, J. J. Heyd, E. N. Brothers, K. N. Kudin, V. N. Staroverov, T. A. Keith, R. Kobayashi, J. Normand, K. Raghavachari, A. P. Rendell, J. C. Burant, S. S. Iyengar, J. Tomasi, M. Cossi, J. M. Millam, M. Klene, C. Adamo, R. Cammi, J. W. Ochterski, R. L. Martin, K. Morokuma, O. Farkas, J. B. Foresman, D. J. Fox, Gaussian, Inc., Wallingford CT, 2016.
- 173. Y. Zhao, D. G. Truhlar, Theor. Chem. Acc., 2008, 120, 215.
- 174. (a) W. J. Hehre, R. Ditchfield, J. A. Pople, *J. Chem. Phys.*, 1972, 56, 2257; (b) P. C. Hariharan, J. A. Pople, *Theor. Chem. Acc.*, 1973, 28, 213; (c) M. M. Francl, W. J. Pietro, W. J. Hehre, J. S. Binkley, D. J. DeFrees, J. A. Pople, M. S. Gordon, *J. Chem. Phys.*, 1982, 77, 3654.
- (a) M. Dolg, U. Wedig, H. Stoll, H. Preuss, *J. Chem. Phys.*, **1987**, 86, 866; (b) J. M. L. Martin, A. Sundermann, *J. Chem. Phys.*, **2001**, 114, 3408.
- 176. (a) G. Scalmani, M. J. Frisch, J. Chem. Phys., 2010, 132, 114110; (b) J. Tomasi, B. Mennucci, R. Cammi, Chem. Rev., 2005, 105, 2999; (c) M. Caricato, J. Chem. Theory & Comput., 2012, 8, 4494.
- 177. (a) E. Runge, E. K. U Gross, *Phys. Rev. Lett.*, 1984, 52, 997. (b) R. Bauernschmitt, R. Ahlrichs, *Chem. Phys. Lett.*, 1996, 256, 454; (c) M. E. Casida, C. Jamorski, K. C. Casida, D. R. Salahub, *J. Chem. Phys.*, 1998, 108, 4439; (d) R. E. Stratmann, G. E. Scuseria, M. J. Frisch, *J. Chem. Phys.*, 1998, 109, 8218; (e) G. Scalmani, M. J. Frisch, B. Mennucci, J. Tomasi, R. Cammi, V. Barone, *J. Chem. Phys.*, 2006, 124, 094107; (f) J. Liu, W. Liang, *J. Chem. Phys.*, 2011, 135, 184111; (g) F. Adamo, D. Jacquemin, *Chem. Soc. Rev.*, 2013, 42, 845.
- 178. The PyMOL Molecular Graphics System, version 2.5.4, Schrödinger, LLC.
- 179. https://gist.github.com/bobbypaton.

VIII.RESULTS DISSEMINATION

VIII.1. List of articles

- D. Dumitraş, E. Gál, C. Silvestru, A. Pop, Complexes Containing Homoleptic Diorganoselenium(II) Ligands: Synthesis, Characterization and Investigation of Optical Properties, *Molecules*, 2024, 29, 792, DOI: 10.3390/molecules29040792, Impact factor (2024): 4.6.
- D. Dumitras, D. Dalmau, P. García-Orduña, A. Pop, A. Silvestru, E. P. Urriolabeitia, Orthopalladated imidazolones and thiazolones: synthesis, photophysical properties and photochemical reactivity, *Dalton Trans.*, 2024, 53, 8948, DOI: 10.1039/D4DT00730A, Impact factor (2024): 3.3.
- 3. <u>D. Dumitras</u>, C. Şalgău, A. Silvestru, Silver(I) complexes with pyridine-based ligands bearing organoselenium groups. *Manuscript in preparation*.

VIII.2. List of conferences

- D. Dumitraş, A. Silvestru, A. Pop, Synthesis, Structural Characterization and Reactivity of New Organoselenium Compounds Containing 4-aryliden-5(4H)-oxazolones – poster, 36th National Chemistry Conference, 4th-7th October 2022, Călimănești-Căciulata, Romania.
- E. P. Urriolabeitia, D. Dalmau, J. V. Alegre-Requena, J. M. Matxain, D. Dumitras, A. Pop,
 A. Silvestru, Fluorescence Amplification in Orthopalladated Azlactones: Experimental,
 Computational and Machine Learning Predictive Studies oral presentation, 29th
 PhotoIUPAC Symposium on Photochemistry, 14th-19th July 2024, Valencia, Spain.
- 3. D. Dumitraș, D. Dalmau, A. Silvestru, E. P. Urriolabeitia, A. Pop, Synthesis, structural characterization and photochemical reactivity of new orthopalladated 4-arylidene-5(4*H*)-thiazolones poster, 11th Workshop of the Selenium and Sulfur Redox and Catalysis Network (WSeS-11), 25th-26th May 2024, Toruń, Poland.
- D. Dumitraş, A. Silvestru, Synthesis, Pyridine Based Organoselenium Compounds. Synthesis, Characterization and Reactivity – oral presentation, 5th Young Researchers' International Conference on Chemistry and Chemical Engineering, 8th-10th May 2025, Cluj-Napoca, Romania.
- 5. D. Dumitraș, A. Silvestru, Group 11 complexes of diorganoselenium ligands containing a 2,6-functionalized pyridine poster, 12th Workshop of the Selenium and Sulfur Redox and Catalysis Network (WSeS-12), 24th-25th August 2025, Jena, Germany.